ChemComm

FEATURE ARTICLE

View Article Online
View Journal | View Issue

Cite this: *Chem. Commun.*, 2016, **52**, 9485

Marriage of heavy main group elements with π-conjugated materials for optoelectronic applications

Sarah M. Parke,† Michael P. Boone† and Eric Rivard*

Received 13th May 2016,
Accepted 20th June 2016

DOI: 10.1039/c6cc04023c

www.rsc.org/chemcomm

This review article summarizes recent progress in the synthesis and optoelectronic properties of conjugated materials containing heavy main group elements from Group 13–16 as integral components. As will be discussed, the introduction of these elements can promote novel phosphorescent behavior and support desirable molecular and polymeric properties such as low optical band gaps and high charge mobilities for photovoltaic and thin film transistor applications.

Introduction

The rich field of organic electronics grew out of a combination of key advances in synthetic organic and polymer chemistry along with a collective desire to obtain lightweight and processable conducting materials for applications ranging from the fabrication of energy efficient LEDs to flexible solar cells.[1–5]

In a similar fashion, a general increase in knowledge as it pertains to inorganic synthesis has spurred renewed interest in π-conjugated materials containing inorganic elements. Highlights of this field include the rapid and extensive development of thiophene-based oligomers and polymers as light harvesting/charge generating species in bulk heterojunction solar cells[6–11] and the use of high charge mobility silicon- and sulfur-based heterocycles in transistors.[12] Furthermore novel luminescence phenomena such as aggregation-induced emission (AIE) are now readily attainable with inorganic heterocycles,[13] while the continual development of inorganic polymers enables access to advantageous redox, flame resistant and self-assembly properties not readily achieved with purely organic polymers.[14–16]

Some challenges that initially slowed progress in heavier main group element (E)-based π-conjugated systems include: the generally high reactivity of E–C bonds due to increased bond polarity and weaker orbital overlap when large/electropositive E atoms are present, and a lack of suitable starting reagents.

Department of Chemistry, University of Alberta, 11227 Saskatchewan Dr., Edmonton, Alberta, Canada T6G 2G2. E-mail: erivard@ualberta.ca; Tel: +1 780-915-4120

† These authors contributed equally.

Sarah M. Parke

Sarah was born in Kelowna, British Columbia, Canada and completed her BSc (Honours) in Chemistry at the University of British Columbia's Okanagan campus in 2014. She is currently working towards her PhD at the University of Alberta under the supervision of Prof. Eric Rivard. Her research interests include the synthesis and polymerization of novel bismuth heterocycles for applications in OLED technologies.

Michael P. Boone

Michael Boone was born and raised in Fort McMurray, Alberta, Canada and obtained his BSc in chemistry from the University of Calgary in 2009. He completed his PhD at the University of Toronto in 2013, under the supervision of Prof. Douglas W. Stephan investigating olefin metathesis catalysis and metal-enhanced Lewis acids and bases for frustrated Lewis pair (FLP) chemistry. In 2015 he undertook an Izaak Walton Killiam postdoctoral fellowship at the University of Alberta, working in the lab of Prof. Eric Rivard and is currently investigating the synthesis of new tellurophene-containing species with extended π-conjugated backbones.

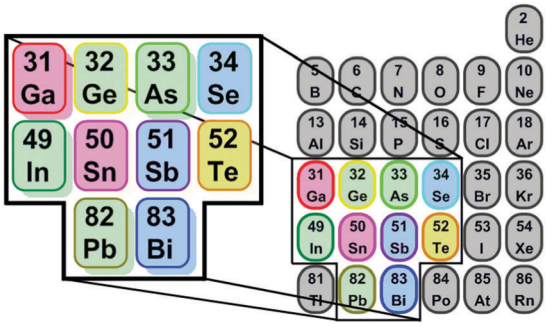

Chart 1 Summary of inorganic elements to be discussed in this review.

However as we will see, the substantial effort devoted to designing new synthetic approaches, such as the use of Zr/E exchange to prepare main group heterocycles,[17] has enabled researchers to push beyond the abovementioned hurdles to achieve the important breakthroughs highlighted in this review. In order to keep the length of this review to a manageable level, only the synthesis and chemistry of π-conjugated systems bearing the heaviest members of the main group (see Chart 1) will be discussed; we will also focus our discussions on compounds that show promising optoelectronic properties. Those interested in learning more about the novel bonding arrangements and reactivity associated with inorganic π-structures, such as heavy element analogues of alkenes,[18–20] alkynes,[21,22] and benzene[23,24] are referred to the excellent review articles that are found in the literature.

Group 13 heterocycles

The incorporation of electron deficient three-coordinate boron centers within extended π-frameworks has led to the development of structurally unique molecules and macromolecules with high Lewis acidities,[25,26] color tunable luminescence,[27–29] and analyte sensing capabilities.[30,31] The corresponding heavier triel element (Al, Ga, In and Tl)-containing congeners have been less explored due to the relative scarcity of known preparative strategies. Fortunately there has been considerable recent progress in this field including the ability to gain access to phosphorescent materials due to increased spin–orbit coupling within heavier elements, which facilitates mixing of singlet and triplet excited states.

Eric Rivard

Eric Rivard obtained his BSc (Hon.) from the University of New Brunswick and a PhD from the University of Toronto under the supervision of Professor Ian Manners. He was then a NSERC PDF with Professors Jonas Peters (Caltech) and Philip Power (UC Davis), and later a research associate with Professor Cameron Jones (Monash University). In 2008 he joined the University of Alberta and is now an Associate Professor. His group actively studies main group element and polymer chemistry with specific interests in inorganic hydrides and the use of metallacycle transfer to create new optoelectronic materials.

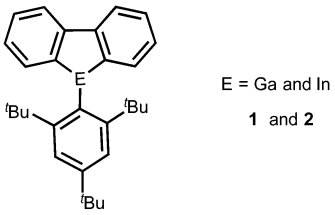

Fig. 1 Original gallafluorene and indafluorene prepared by Cowley and coworkers.

Gallium

In 1995, Cowley *et al.* reported the synthesis of the highly moisture-sensitive gallafluorene and indafluorene (**1** and **2**) which contained the kinetically stabilizing 2,4,6-$^{t}Bu_3C_6H_2$ (Mes*) group at the respective heteroatom (Fig. 1).[32] Following a similar strategy as used to prepare borafluorenes[25,26,33,34] these Ga and In heterofluorenes were prepared by a general salt elimination reaction between 2,2′-dilithiobiphenyl and Mes*ECl_2 (E = Ga and In). The molecular structure of **1** was determined by X-ray crystallography, however no supporting optical or electrochemical studies were reported for either species.

A significant advance in the field of gallium heterocycles emerged in 2013 when a series of gallafluorenes (**3–8**) were prepared by the Chujo group (Scheme 1).[35,36] In order to achieve enhanced stability to water, a modified Mes*-type ligand (Mamx) was employed, wherein an *ortho-tert*-butyl group was replaced by a coordinating $-CH_2NMe_2$ unit. Several Mamx gallafluorene derivatives were synthesized according to the salt elimination/post Suzuki–Miyaura cross-coupling protocol shown in Scheme 1.

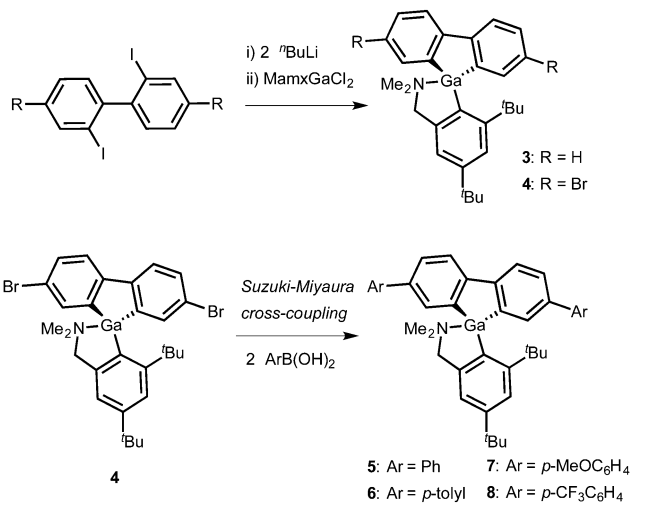

Scheme 1 Synthesis of the luminescent Mamx gallafluorene derivatives **5–8**.

Emission in the near UV (λ_{em} = 369 nm; $\phi < 0.01$) was noted for the parent gallafluorene **3** while the π-extended congeners **5–8** displayed slightly red-shifted emission (λ_{em} in the range of 385 to 395 nm) and increased quantum yields (ϕ = 0.29–0.36). These species adopt four-coordinate Ga environments in the solid state as determined by X-ray crystallography. Addition of the strong Lewis acid $B(C_6F_5)_3$ into solutions of the gallafluorenes **3** and **5–8** afforded new products with red-shifted emission luminescence in comparison to the borane-free gallafluorenes [*e.g.* λ_{em} = 575 nm for **3**·$B(C_6F_5)_3$; λ_{em} = 635–684 nm for **5–8**·$B(C_6F_5)_3$, respectively]. Furthermore these $B(C_6F_5)_3$ adducts have significantly longer emission lifetimes of up to 1.33 μs *vs.* <5 ns for the uncomplexed gallafluorenes; thus visible phosphorescence could be turned on by coordinating $B(C_6F_5)_3$ to a $-CH_2NMe_2$ group within the Mamx ligand scaffold. Under low concentrations of **3** and $B(C_6F_5)_3$ the phosphorescence emission peak at 575 nm disappeared, indicating that the Mamx-$B(C_6F_5)_3$ coordinative interaction is reversible in nature. As expected, introduction of oxygen to **3**·$B(C_6F_5)_3$ resulted in the disappearance of the 575 nm band due to O_2-triggered phosphorescence quenching.[37] The wavelength of phosphorescence could be shifted even further towards the near IR spectral region by incorporating more electron-donating the substituents about the periphery of the gallafluorene unit (*e.g.* λ_{em} for **7**·$B(C_6F_5)_3$ = 684 nm).[35]

Chujo *et al.* expanded on their previous studies to obtain stable gallafluorene polymers.[38] It was found that monomer **4** could participate in various palladium-catalyzed C–C bond-forming protocols including Suzuki–Miyaura, Stille, and Sonogashira cross-coupling (Scheme 2). As a result, these methods could each be used to gain access to copolymers featuring Mamx-functionalized gallafluorene repeat units in combination with a wide range of different π-conjugated comonomers. Despite the low number of repeating units in these first generation polymers (*e.g.* 6–13) many of these Ga-containing polymers exhibited impressive thermal stability (up to 300 °C in air). Furthermore color tunable photoluminescence that ranged from UV to visible red emission was possible for polymers **9–15** shown in Scheme 2. Cyclic voltammetry (CV) of these gallafluorene polymers identified higher lying HOMO and LUMO levels in comparison to their carbon-based analogues,[39–42] suggesting that these novel gallafluorene polymers could be used as hole transport materials. Band gap narrowing *via* lowering of LUMO levels was possible by incorporating electron deficient benzotriazole (**14**) and benzothiadiazole (**15**) units to yield donor–acceptor motifs, thus opening the door for possible solar cell applications. By judicious choice of ligand/base for cross-coupling polymerization, it is expected that higher molecular weight materials could be prepared in the near future.

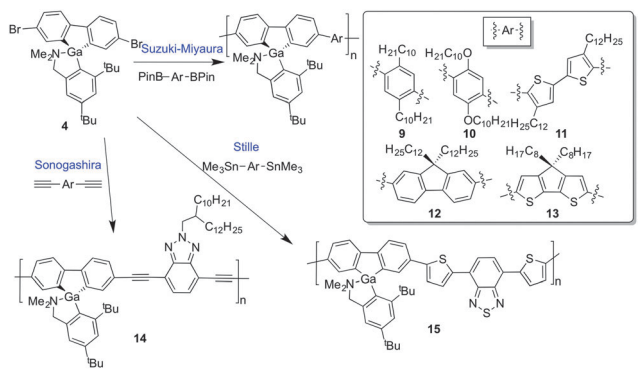

Scheme 2 Synthesis of polygallafluorenes by palladium-mediated cross-coupling.

Indium

Early examples of well-characterized indium heterocycles (Fig. 2) were made by Peppe and Tuck who reported the synthesis of the pyridine (pyr) adduct Ph_4C_4InCl·pyr (**16**) as well as a $[Ph_4As]^+$ salt of the anionic spirocycle $\{[Ph_4C_4]_2In\}^-$ (**17**);[43] the optoelectronic properties of these interesting heterocycles have yet to be examined.

The Chujo group built upon their initial gallafluorene studies outlined in Schemes 1 and 2 to include four-coordinate boron-, aluminum- and indium-based heterofluorenes containing the Mamx ligand (Fig. 3).[44] Planar arrangements were found in each heterofluorene substructure with UV-vis spectroscopy revealing similar λ_{max} (*ca.* 280 nm) and molar extinction coefficients (ε = 7.9 to 8.9 × 10^3 M^{-1} cm^{-1}) in each species. TD-DFT calculations revealed that the 280 nm absorptions arose from π–π* transitions within a biphenyl unit, and thus are not significantly influenced by the nature of the heteroatom present. Comparative photoluminescence studies of the B, Al, Ga and In analogues were made at both room temperature and at 77 K. At room temperature the B, Al, and Ga heterofluorenes (**18**, **19**, and **3**) exhibited near UV fluorescence centered at 360 nm with emission lifetimes (τ) of less than 5 ns; the In congener (**20**) also yielded an additional phosphorescence-based emission band around 490 nm (τ > 50 μs) that was quenched in air. Upon cooling compounds **3**, **18–20** to 77 K in 2-MeTHF, emission bands at *ca.* 330 and 480–490 nm were found in each case. The authors also noted that the proportion of phosphorescence

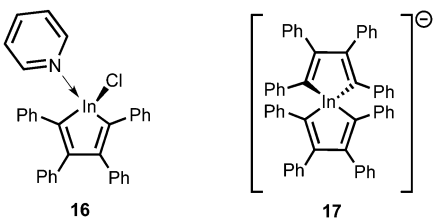

Fig. 2 First well-characterized indium heterocycles reported by Peppe and Tuck.

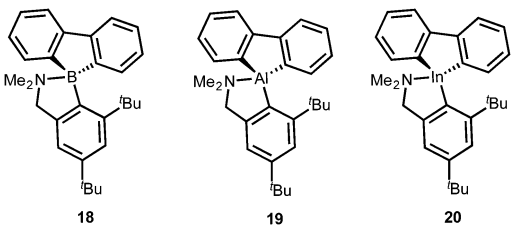

Fig. 3 Isostructural luminescent Mamx-heterofluorenes reported by Chujo.

in relation to the total light emitted increased within the heavier Group 13 heteroles, and correlated with the larger spin–orbit coupling constants ζ on going from B to Al to Ga to In (10 to 62 to 464 to 1183 cm^{-1}),[45] thus phosphorescence was modulated by the heavy atom effect.

Group 14 element heterocycles

Since the establishment of the field of organoelectronics, many have sought to prepare heavier Group 14 element analogues to gain a deeper understanding of aromaticity and to obtain potentially advantageous optoelectronic properties. Perhaps the most well-studied Group 14 element based heterocycles are five-membered siloles. Initial motivation for examining these species was to determine if significant Si–R σ^*/C=C π^* orbital mixing could transpire to lower the LUMO state and the overall electronic band gap in relation to organic cyclopentadienes.[46] While both monomeric and polymeric siloles (and their structural analogues) are still being explored as viable constructs for photovoltaic and TFT applications[47–49] there has been a surge in interest in arylated siloles, such as hexaphenylsilole $Ph_4C_4SiPh_2$, due to their ability to show aggregation-induced emission (AIE) of visible light. In AIE, molecular rotations that normally facilitate non-radiative decay in the excited state are suppressed by the aggregation-induced restriction of molecular motion.[50] Accordingly a large number of silole analogues have been prepared for applications such as LED development, two-photon bioimaging and the sensing of analytes.[50–53] Herein we will describe key advances in the domain of formally conjugated heterocycles containing Ge, Sn and Pb.

Germanium

The presence of germanium in optoelectronic devices dates back to its use in first-generation transistors. More recent studies have focused on incorporating germanium within potentially conjugated frameworks for optoelectronic applications ranging from the development of polymer-based bulk heterojunction solar cells (BHJSCs) and light-emitting materials. The most commonly studied molecular group within the field of Ge heterocycles are five-membered germoles such as the prototypical species hexaphenylgermole $Ph_2GeC_4Ph_4$. A driving force behind studying these materials is to take advantage of possible σ^*–π^* mixing within these heterocycles leading to lower LUMO states;[54] aggregation-induced emission from germoles was also reported by Braddock-Wilking and coworkers.[55] Recent work on germoles and their ring-fused analogues will be covered below with topic grouping arranged according to the noted optoelectronic properties, due to the large size of this research domain.

Bulk heterojunction solar cells

As mentioned, many have sought to incorporate inorganic elements within photovoltaically active polymers to gain access to potentially lower optical band gaps, enhanced light absorption, and improved charge carrier mobilities.[1] One successful way to achieve narrower electronic band gaps is a donor–acceptor approach which places electron-rich and electron-poor heterocycles in an alternating fashion along a polymer backbone,[56] with fused germanium-containing heterocycles often acting as electron-donors.[9] Accordingly there has been a flurry of activity over the past several years to incorporate ring-fused germoles into polymers as the electron-donors, as will be discussed below.

The most widely studied germanium-based π-conjugated framework in BHJSCs is dithienogermole, which has been copolymerized with a wide range of electron-deficient monomers (Fig. 4; **21–41**).[57–72] The dithienogermole-containing polymers (**21–41**) are generally obtained by metal-catalyzed cross-coupling methodologies such as the Stille, Suzuki–Miyaura and Sonogashira reactions, and very high number average molecular weights (M_n) of up to 133 000 g mol^{-1} have been occasionally reported. Due to d-block contraction,[73,74] the electronegativity of germanium is slightly closer to carbon than the related silicon species,[75] therefore reducing the polarization of the Ge–C bond and rendering aryl germanes more tolerable towards bases and nucleophiles than the related aryl silanes.[76,77]

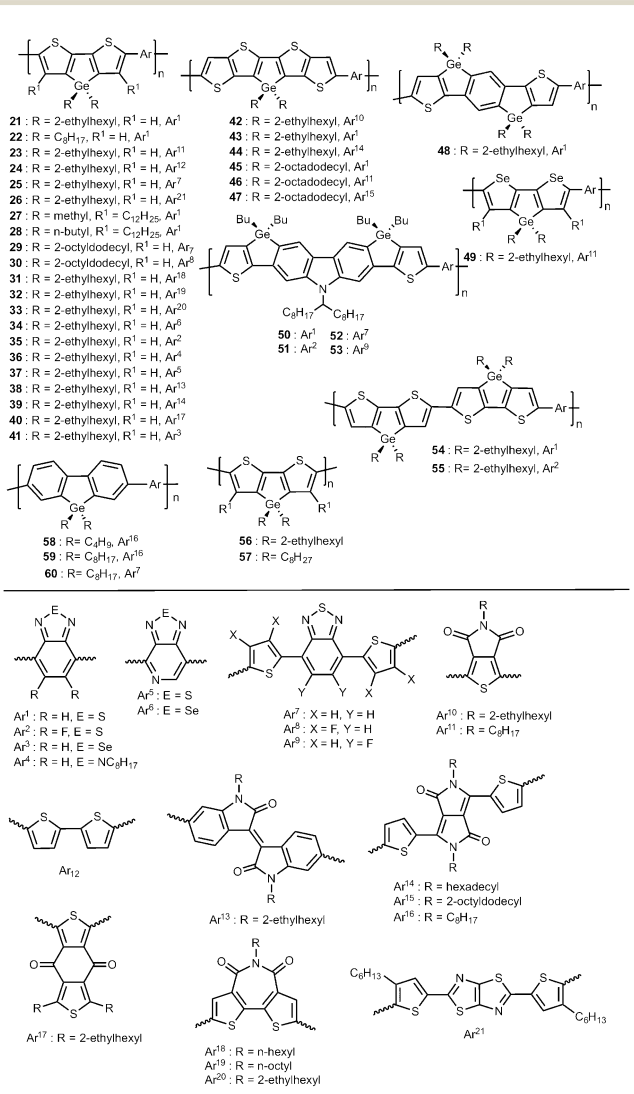

Fig. 4 Various germanium-containing conjugated polymers (**21–60**).

Table 1 Photovoltaic data for compounds **21–60**. $PC_{70}BM$ = [6,6]-phenyl-C_{70}-butyric acid methyl ester; $PC_{71}BM$ = [6,6]-phenyl-C_{71}-butyric acid methyl ester; CN = 1-chloronaphthalene; DIO = 1,8-diiodooctane; V_{OC} = open circuit voltage; J_{SC} = short circuit current; FF = fill factor; PCE = power conversion efficiency

Entry	Compound	Ref.	M_n (g mol^{-1})	PDI	Blended with	Blend ratio	Additive	V_{OC} (V)	J_{SC} (mA cm^{-2})	FF (%)	PCE (%)
1	**21**	87	31 000	3.16	$PC_{70}BM$	1 : 1	CN (3%)	0.57	18.60	43.0	4.50
2	**22**	92	8900	1.9	$PC_{70}BM$	N/A	N/A	0.53	7.80	36.0	1.50
3	**23**	58	16 300	1.9	$PC_{70}BM$	N/A	DIO (5%)	0.86	14.70	64.5	8.20
4	**24**	65	10 000	2.7	$PC_{70}BM$	1 : 3.6	N/A	0.54	2.52	62.0	0.84
5	**25**	66	3800	3.15	$PC_{70}BM$	1 : 3.6	DIO	0.59	5.47	48.0	1.55
6	**26**	66	11 000	2.34	$PC_{70}BM$	1 : 3.6	DIO	0.58	6.31	65.0	2.38
7	**27**	68	22 400	1.78	$PC_{70}BM$	1 : 4	N/A	0.94	6.11	46.0	2.66
8	**28**	68	54 700	1.74	$PC_{70}BM$	1 : 4	N/A	0.90	3.71	45.0	1.50
9	**29**	69	39 000	2.5	$PC_{71}BM$	1 : 2	N/A	0.66	7.46	68.0	3.51
10	**30**	69	37 000	2.8	$PC_{71}BM$	1 : 2	N/A	0.71	13.51	57.0	5.47
11	**31**	70	27 000	2.9	$PC_{71}BM$	1 : 1	DIO (3%)	0.77	12.30	50.2	4.77
12	**32**	70	25 000	2.7	$PC_{71}BM$	1 : 1.5	DIO (3%)	0.75	12.17	47.2	4.32
13	**33**	70	18 000	2.3	$PC_{71}BM$	1 : 1	DIO (3%)	0.77	10.09	46.7	3.62
14	**34**	63	5700	1.5	$PC_{70}BM$	1 : 3.6	DIO (2.5%)	0.31	2.02	29.0	0.18
15	**35**	67	8000	1.51	$PC_{70}BM$	1 : 2	N/A	0.67	5.74	54.0	2.10
16	**36**	67	23 000	1.16	$PC_{70}BM$	1 : 2	N/A	0.70	6.17	56.0	2.40
17	**37**	67	24 000	1.36	$PC_{70}BM$	1 : 2	DIO (2.5%)	0.59	19.60	57.0	6.60
18	**38**	72	133 000	3.88	$PC_{71}BM$	1 : 1	DIO (3%)	0.84	10.70	45.5	4.07
19	**39**	72	6850	1.5	$PC_{71}BM$	1 : 2	DIO (3%)	0.52	3.19	63.6	1.05
20	**40**	72	24 200	2.52	$PC_{71}BM$	1 : 3	DIO (7%)	0.94	10.30	65.0	6.28
21	**41**	71	15 600	1.99	$PC_{71}BM$	1 : 1	DIO (0.5%)	0.48	9.48	44.3	2.02
22	**42**	79	12 000	1.4	$PC_{71}BM$	1 : 2	N/A	0.81	13.85	64.0	7.16
23	**43**	80	10 000	3.5	$PC_{71}BM$	1 : 2	N/A	0.71	14.04	47.0	4.66
24	**44**	80	32 000	2.0	$PC_{71}BM$	1 : 2	N/A	0.69	3.56	35.0	0.87
25	**45**	80	26 000	3.4	$PC_{71}BM$	1 : 2	N/A	0.79	7.30	35.0	2.04
26	**46**	80	36 000	1.8	$PC_{71}BM$	1 : 2	N/A	0.88	3.71	63.0	2.06
27	**47**	80	75 000	2.0	$PC_{71}BM$	1 : 2	N/A	0.69	2.56	66.0	1.16
28	**48**	82	37 000	1.3	$PC_{71}BM$	1 : 3.5	N/A	0.85	13.95	55.0	6.50
29	**49**	93	41 000	1.5	$PC_{71}BM$	1 : 2	DIO (3%)	0.74	12.10	58.0	5.20
30	**50**	94	55 200	1.78	$PC_{71}BM$	1 : 3	N/A	0.80	8.44	44.9	3.03
31	**51**	94	22 000	1.35	$PC_{71}BM$	1 : 4	N/A	0.90	4.27	51.1	1.96
32	**52**	94	26 800	1.7	$PC_{71}BM$	1 : 2	N/A	0.76	5.78	37.3	1.63
33	**53**	94	17 900	1.73	$PC_{71}BM$	1 : 4	N/A	0.84	11.19	47.7	4.50
34	**54**	85	N/A	N/A	$PC_{71}BM$	1 : 2.5	N/A	0.53	12.69	64.0	4.30
35	**55**	85	13 000	1.2	$PC_{71}BM$	1 : 2.5	N/A	0.60	3.66	43.0	0.94
36	**56**	64	46 000	1.6	$PC_{70}BM$	1 : 3.6	DIO (2.5%)	0.50	5.09	67.0	1.71
37	**57**	64	79 000	2.7	$PC_{70}BM$	1 : 3.6	DIO (2.5%)	0.36	6.35	56.0	1.28
38	**58**	86	13 000	2.8	$PC_{70}BM$	N/A	N/A	0.76	4.10	62.0	1.50
39	**59**	86	14 000	3.5	$PC_{70}BM$	N/A	N/A	0.76	2.80	56.0	1.20
40	**60**	86	10 000	2.4	$PC_{70}BM$	N/A	N/A	0.79	6.90	51.0	2.80

This in turn allows for the utilization of Suzuki–Miyaura cross-coupling protocol while avoiding toxic tin-based Stille cross-coupling, enabling much deeper investigation into these germole-containing polymers. While various dithienogermoles have been incorporated in solar cells with power conversion efficiencies (PCEs) ranging from 0.18% to 8.2% (Table 1, entries 1–21), it should be stated that Reynolds, So and coworkers were the first to incorporate a polydithienogermole (**23**) into a BHJ solar cell (in 2011).[57] The same team also conducted further device optimizations leading to a record PCE in this subfield of 8.2% for **23** (Table 1, entry 3) when thicker active layers comprised of the polymer donor and fullerene acceptor ($PC_{71}BM$) were used.[58] Related high performing devices were achieved by Heeney, Fei, Chochos and coworkers[67] including the dithienogermole–azabenzothiadiazole copolymer **37** which yielded a PCE value of 6.6% (Table 1, entry 17). Similarly, Hou and coworkers[72] fabricated a device based on the dithienogermole–benzoselenodiazole copolymer **40** that provided a PCE of 6.3% (Table 1, entry 20). It should be mentioned that the devices mentioned in entries 3, 17 and 20 in Table 1 all utilized the additive 1,8-diiodooctane (DIO) which typically helps reduce the phase separation between the electron-donor (the germanium-containing polymers) and the electron-accepting the fullerenes, $PC_{70}BM$ or $PC_{71}BM$.[57,78] Heeney and coworkers[69] prepared a functional BHJSC utilizing **30** that was able to achieve a modest PCE of 5.5% (Table 1, entry 10), which was the highest efficiency found without the use of any additives for these dithienogermoles.

In order to potentially capture more incident photons in the near IR region by narrowing the polymer band gap, Heeney and coworkers[79,80] prepared extended ring-fused electron-donor cores comprised of thieno[3,2-*b*]thiophene heterocyclic units bridged by –GeR_2– residues, and copolymerized these dithienogermolodithiophene units with a variety of electron-acceptors to yield copolymers **42–47** (Fig. 4). These polymers had molecular weights ranging from 10 000 to 75 000 g mol^{-1} and PCEs spanning from 0.8% to a value of 7.2% for **42** (Table 1, entries 22–27); each device was fabricated without additives. Heeney and coworkers also developed a novel germaindacenodithiophene building block to synthesize the benzothiadiazole

copolymer **48**.[81] Later Ashraf, Schroeder and coworkers[82] were able to increase the efficiency of additive-free devices featuring high molecular weight **48** (M_n = 37 000 g mol^{-1}) to yield a PCE of 6.5% (Table 1, entry 28). The Heeney group also developed devices utilizing an analogous polymer with a more electron-rich diselenogermole core (**49**; Fig. 4), however despite the high molecular weight of the material (41 000 g mol^{-1}), a slightly reduced PCE of 5.2% was found when using DIO as an additive (Table 1, entry 29).[26] This study highlights a common challenge in the field, which is the role of morphological/interfacing effects in dictating BHJSC performance.[83] In 2014, Cheng and coworkers introduced a new dithienogermolocarbazole unit to the area, and the reported copolymers **50–53** (Fig. 4) also gave moderate PCE values of up to 4.5% (Table 1, entries 30–33).[84]

Ohshita and coworkers have explored in depth the influence of dithienogermole repeat units on solar cell device performance, and in one study they incorporated two of these frameworks into every repeat unit to make polymers **54** and **55** (Fig. 4).[85] Unfortunately, polymer **54** was not soluble enough to enable molecular weight characterization by gel permeation chromatography (GPC), however **55** was obtained with a M_n of 13 000 g mol^{-1} (polydispersity index, PDI = 1.2). Despite the enhanced solubility of **55**, this polymer afforded a device with a much lower PCE value (0.9%) in comparison to its less soluble counterpart **54** (PCE = 4.3%; Table 1, entries 34 and 35). The same group also prepared alkyl-functionalized dithienogermole homopolymers (**56** and **57**; Fig. 4) with high molecular weights *via* Stille coupling (M_n = 46 000 and 79 000 g mol^{-1}, respectively), although their performances in BHJSC architectures was modest (PCE = 1.7 and 1.3%, respectively; Table 1, entries 36 and 37).[64]

The Leclerc group has had a key role in advancing the use of germanium-containing polymers for optoelectronic applications[86] beginning with the development of a series of polymers (**58–60**; Fig. 4) containing electron-rich germafluorene units. These polymers were obtained with number average molecular weights (M_n) in the range of 10 000–13 000 g mol^{-1} and moderate PCE values for solar cells devices from 1.2 to 2.8% in the absence of any additives. Germafluorenes also show stable blue light emission for LED applications, and more detail on this growing field will be provided later in this review.

Transistors and semi-conducting materials

While germanium-containing π-materials have been extensively explored as donor-materials in BHJSCs, the use of germanium heterocycles within thin film transistors (TFTs) has been less studied with recent examples outlined in Table 2.[63,69,85–90] The previously mentioned polymer **21** originally synthesized by Heeney and coworkers was also examined as a component of TFTs with a promising mobility of 0.11 cm^2 V^{-1} s^{-1} noted.[87] Similarly, the previously described dithienogermole and germafluorene copolymers **54–60** (Fig. 4) were also incorporated into TFT devices (Table 2, entries 2–8), however in each case relatively low mobilities were noted, with **58** having the highest value at 0.04 cm^2 V^{-1} s^{-1} amongst the series (with a notably high on/off ratio of *ca.* 1 × 10^6).[64,85,86]

Several other germanium-containing polymers were also investigated for TFT applications (Fig. 5; polymers **61–69**).

Table 2 TFT data for compounds **21**, and **54–69**. BC = bottom-contact; TC = top-contact; TG = top-ground; BG = bottom-ground; μ = hole mobility (saturated mobilities); V_T = threshold voltage

Entry	Comp.	Ref.	Device architecture	μ (cm^2 V^{-1} s^{-1})	On/off ratio	V_T (V)
1	**21**	87	TG/BC	0.11	N/A	N/A
2	**54**	85	BG/BC	3.8 × 10^{-3}	1.0 × 10^5	N/A
3	**55**	85	BG/BC	1.4 × 10^{-4}	1.0 × 10^4	N/A
4	**56**	63	BG/BC	3.7 × 10^{-4}	1.0 × 10^3	N/A
5	**57**	63	BG/BC	1.9 × 10^{-4}	1.0 × 10^4	N/A
6	**58**	86	TG/TC	0.04	1.0 × 10^6	−27
7	**59**	86	TG/TC	7.7 × 10^{-3}	3.6 × 10^5	−27
8	**60**	86	TG/TC	1.1 × 10^{-4}	1.8 × 10^4	−26
9	**61**	91	BG/TC	3.2 × 10^{-4}	4.4 × 10^3	−11
10	**62**	91	BG/TC	4.0 × 10^{-4}	3.2 × 10^2	−8.3
11	**63**	88	BG/BC	0.55	9 × 10^5	N/A
12	**64**	89	TG/BC	6.2 × 10^{-2}	N/A	N/A
13	**65**	89	TG/BC	2.8 × 10^{-3}	N/A	N/A
14	**66**	90	TG/BC	0.036	N/A	N/A
15	**67**	90	TG/BC	8.0 × 10^{-4}	N/A	N/A
16	**68**	90	TG/BC	4.6 × 10^{-3}	N/A	N/A
17	**69**	90	TG/BC	0.26	N/A	N/A

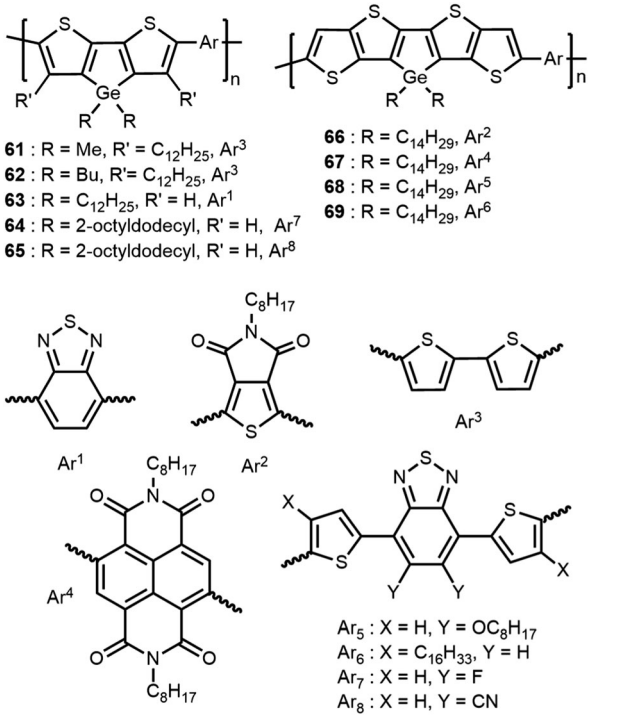

Fig. 5 Structures of compounds **61–69**.

For example, Heeney *et al.*[91] developed the dithienogermole–bithiophene copolymers **61** and **62**, however both materials displayed low mobilities when incorporated into devices (3.2 × 10^{-4} and 4.0 × 10^{-4} cm^2 V^{-1} s^{-1}, respectively; Table 2, entries 9 and 10). Reynolds and coworkers[88] later showed that the dithienogermole–benzothiadiazole copolymer **63** afforded a TFT with a promising mobility of 0.55 cm^2 V^{-1} s^{-1} and a high on/off ratio near 10^6 (Table 2, entry 11). Heeney and coworkers[89] also studied the dithienogermole-containing polymers **64** and **65** as components of TFTs. Polymers with dithienogermolodithiophene

repeat units (**66–69**) were also tested in TFTs (Table 2, entries 14–17),[90] with occasionally high mobilities recorded (*e.g.* 0.26 $cm^2\ V^{-1}\ s^{-1}$ for **69**).

Light emitting materials

In important early work in this field Tamao and coworkers synthesized the germole **70** according to the multi-step procedure outlined in Scheme 3.[73] In the initial step of the procedure, cyclization of a thiophene-capped diyne with Negishi's reagent ("Cp_2Zr"; prepared from Cp_2ZrCl_2 and two equiv. of ^{n}BuLi)[95] afforded a five membered zirconacycle; this species subsequently underwent Zr/Ge atom exchange with Et_2GeCl_2 to yield the target germole. Compound **70** absorbs maximally at 405 nm, while blue fluorescence was found with an emission maximum (λ_{em}) at 479 nm (relative quantum yield ϕ = 8.7%). The Tilley group also prepared a series of germoles (**71–73**) (Scheme 3)[96] using the thermally stable "Cp_2Zr" source [$Cp_2Zr(Me_3SiCCSiMe_3)$(pyr)].[97] The halogen-capped germoles **71** and **72** (Scheme 3) could be polymerized to yield the polymer **74** *via* nickel-mediated homocoupling.[96] The monomeric germoles **71–73** absorbed light maximally in the narrow spectral range of 364–376 nm, while similar blue light emission as in Tamao's compound **70** was noted [λ_{em} = 452 to 464 nm; relative quantum yields of 8, 12 and 18% for **71**, **72** and **73**, respectively]. Polymer **74** was also obtained with three different M_n values of 1900, 4700 and 20 000 g mol^{-1} and, as expected, the highest molecular weight material afforded the most red-shifted absorption (λ_{max} = 442 nm) and emission (λ_{em} = 500 nm) consistent with enhanced heterocycle coplanarity/conjugation; notably, the highest relative quantum yield (ϕ = 79%) was found with the polymer of M_n = 20 000 g mol^{-1}.

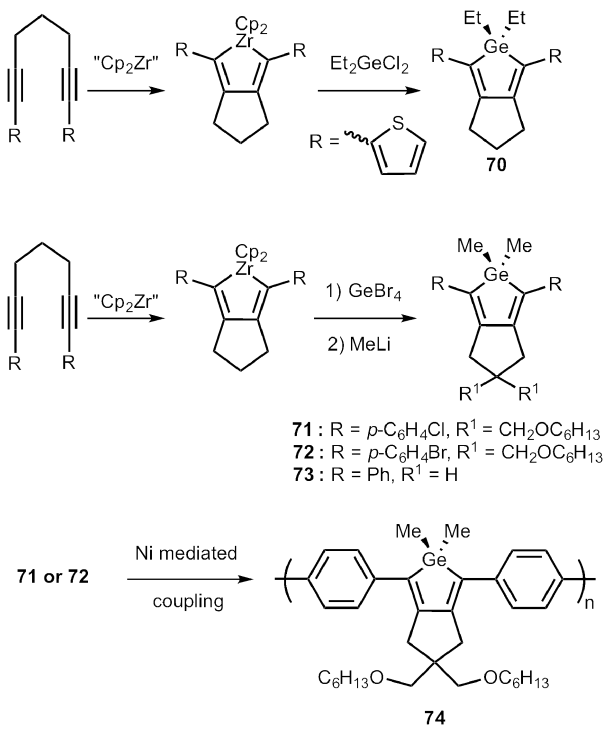

Scheme 3 Synthesis of the germoles **71–73** and the polydiarylgermole **74**.

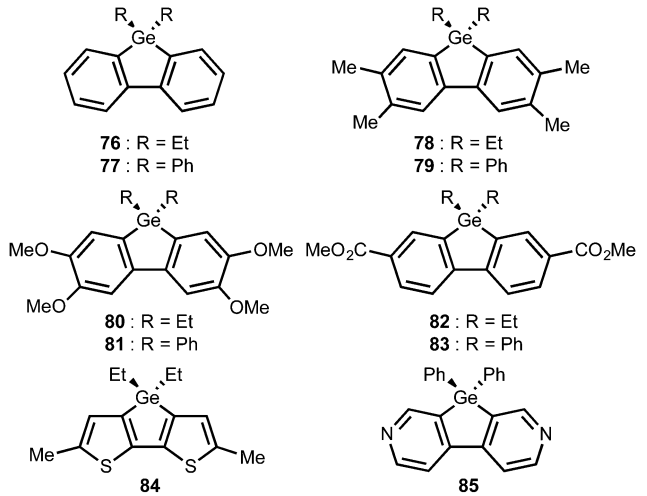

Fig. 6 Structures of **76–85**.

Mullin and coworkers[98] studied hexaphenylgermole, $Ph_2GeC_4Ph_4$ **75**, and noted aggregation-enhanced emission (AEE) in the blue spectral region (λ_{em} at 487 nm) in the solid state when irradiated at *ca.* 357 nm. In line with the AEE effect, the quantum yield of **75** increased from a value of *ca.* 1% in solution to 10% in the solid state. A related effect was noted by Tang and coworkers in their poly(phenylenesilole)s.[99,100]

In 2010 Yamanoi, Nishihara and coworkers[101] were able to synthesize a series of eight germafluorenes (**76–83**) and one dithienogermole (**84**) that were all blue luminescent at room temperature (λ_{em} = 345 to 420 nm) when excited with near UV-vis light (285 to 340 nm) (Fig. 6). The highest quantum yield was found with the dithienogermole **84** with a relative quantum yield of 34% (*vs.* anthracene as a standard). In a related study by Ohshita and coworkers[102] the dipyridinogermole **85** was prepared by treating 2,2′-dilithio-4,4′-bipyridyl with Ph_2GeCl_2. This compound was found to have a λ_{max} at 269 nm and discernable blue fluorescence at 400 nm with a corresponding quantum yield of less than 2%, as determined using an integrating sphere.

One strategy being explored in the field of luminescent fluorenes and their heavier element congeners is to fuse two fluorenyl units to afford spirocyclic arrangements (Scheme 4); the goal is to possibly improve the thermal stability and solubility of these materials for LED fabrication.[103] Accordingly the Ohshita group prepared the spirobi(dithienogermole) **86** (Fig. 7) and this species was found to have a similar absorption profile (λ_{max} at 358 nm) as the corresponding monocyclic

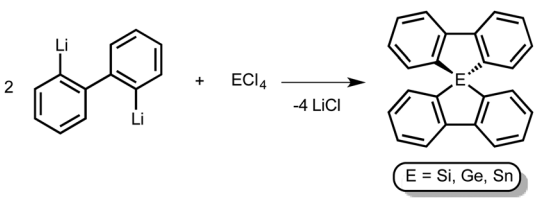

Scheme 4 General synthetic protocol for Group 14 element spirofluorenes.

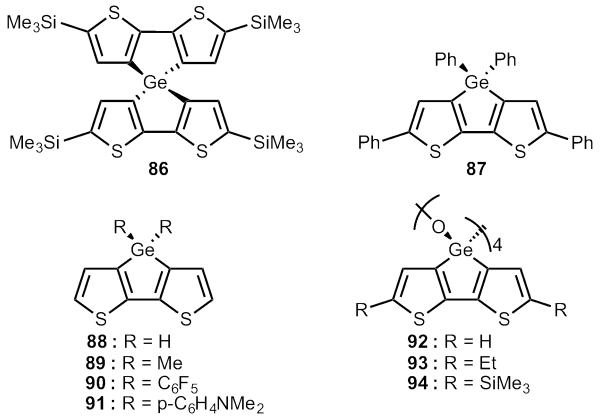

Fig. 7 Various dithienogermoles (**86–94**).

dithienogermoles, suggesting a lack of substantial electronic communication between the fused dithienogermole rings. This compound was also photoluminescent (λ_{em} = 421 nm; ϕ = 0.09) and showed thermal stability above 300 °C.[104] In related work, Adachi, Yasuda and coworkers synthesized the π-extended dithienogermole **87** and found red-shifted absorption (λ_{max} = 401 nm) and emission (λ_{em} at 483 nm) relative to the spirocycle **86**.[105] Compound **87** was also incorporated into an OLED device with an overall device efficiency for blue electroluminescence of 3.4%. In addition to several germanium-substituted dithienogermoles (**88–91**), a number of oxo-bridged dithienogermole tetramers were also synthesized by the Ohshita group (**92–94**, Fig. 7) and a photoluminescent quantum yield of 80% (λ_{em} = 482 nm) was noted in one analogue (**94**).[106]

The Rivard group also prepared a series of spirocyclic germafluorene–germoles (SGGs; **95–98**) with the assistance of zirconium-mediated alkyne coupling, followed by Zr/Ge metathesis chemistry (Scheme 5).[107] Spirocyclic functionality was introduced

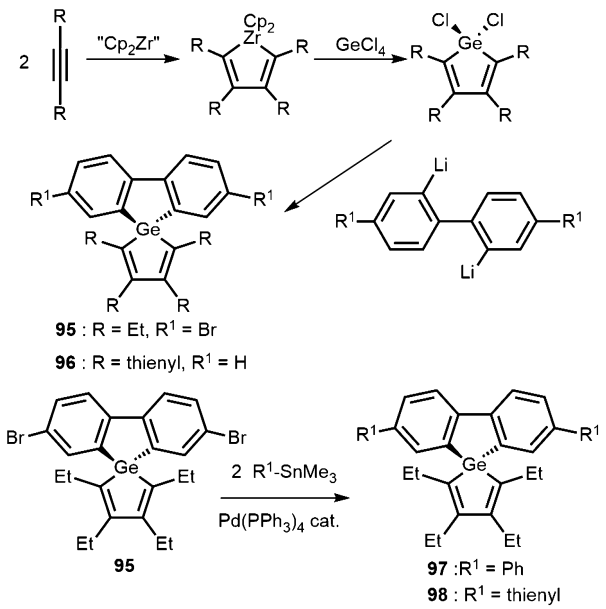

Scheme 5 Synthesis of spirocyclic germafluorene–germoles.

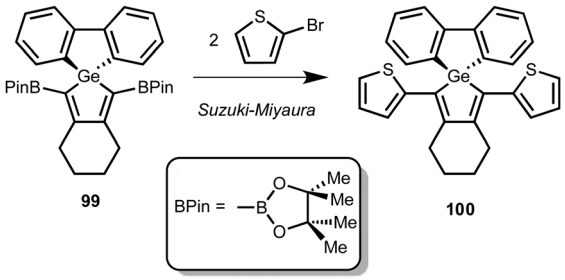

Scheme 6 Suzuki–Miyaura cross-coupling of **99** with 2-bromothiophene.

by reacting dihalogermoles (Scheme 5) with dilithiobiphenyl analogues, and the resulting products exhibited color tunable luminescence: blue emission possible from the germafluorene units, while orange aggregation-induced emission (AIE) was possible from the tetraarylated germole units (*e.g.* in **96**). In addition the thiophene-capped SGGs have substantial photoluminescence stability in air, making this a promising structural class for use in non-encapsulated LEDs. The authors also reported that the functionalized SGG **99** can undergo post-functionalization by Suzuki–Miyaura cross-coupling (Scheme 6) to yield **100** and other π-extended frameworks.[107]

Seferos and coworkers studied the photoluminescent properties of the previously mentioned dithienogermole–benzochalcogenodiazole copolymers **21** and **41** (Fig. 4).[108] Polymer **21** was found to exhibit two visible light absorptions at 405 and 662 nm, while near IR emission was found at λ_{em} = 730 nm. The related benzoselenodiazole polymer **41** exhibited red-shifted absorption (λ_{max} = 422 and 694 nm) and emission profiles (λ_{em} = 795 nm). It would be interesting to see the effect of incorporating tellurium into these polymeric structures and if phosphorescence in the IR spectral region could be achieved; this is a highly sought property for bioimaging applications where interference with background absorption would be minimized.[109] In a recent study, Uhl, Würthwein and coworkers reported the synthesis and photoluminescent properties of the germacyclobutenes **101–106** (Fig. 8).[110] Upon excitation of **103** at *ca.* 265 nm, deep blue fluorescence in the solid state and solution was noted.

Tin

The first report of heavy Group 14 and 15 cyclopentadienyl analogues was by Leavitt, Manuel, and Johnson in 1959.[111] Starting from dilithiotetraphenylbutadiene, they performed condensation reactions with Ph_xECl_2 (E = P, As, Sb, Ge, or Sn; x = 1 or 2) to generate the corresponding heteroles ($Ph_xEC_4Ph_4$). In 1960 the first dibenzostannoles (**107** and **108**) were synthesized from the reaction of dilitihiobiphenyl with Ph_2SnCl_2 and Et_2SnCl_2, respectively (Scheme 7).[112]

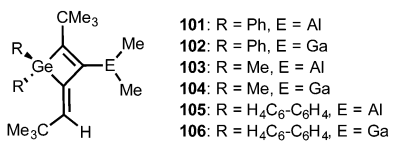

Fig. 8 Structures of the germacyclobutenes **101–106**.

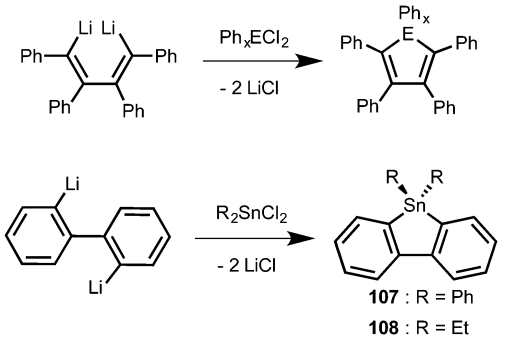

Scheme 7 Synthesis of the stannafluorenes **107** and **108** by salt elimination.

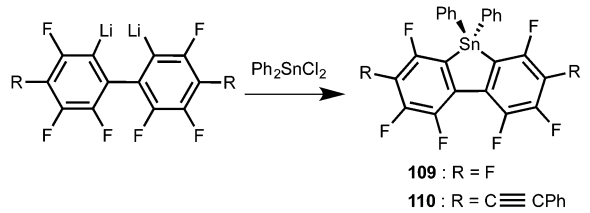

Scheme 8 Synthesis of the perfluorostannafluorenes **109** and **110**.

One versatile method for the construction of electron deficient heterofluorenes is co-condensation of fluorinated dilithiobiphenyls with element dihalides (Scheme 8); one caveat is that lithiated fluoroaromatics need to be handled with care and at low temperatures due to possibly violent decomposition instigated by LiF elimination/benzyne formation.[113] Using this approach Tilley *et al.* prepared a number of structurally related Si, S, P, Ge and Sn-containing heterofluorenes and studied their optoelectronic properties in detail.[114] Of note for this current review, the stannafluorenes (**109** and **110**; Scheme 8) were prepared according to a general procedure developed previously by Cohen and coworkers.[115,116] While compound **109** was non-emissive, placement of phenylethynyl (–C≡CPh) substituents at the 2- and 7-positions of the stannafluorene ring (to give **110**) resulted in a red-shift in the absorption from 309 nm in **109** to 350 and 363 nm for **110**, consistent with an increase in the extent of conjugation. In addition compound **110** yields blue-colored fluorescence both in solution (THF: λ_{em} = 389 and 410 nm) and in the solid state (λ_{em} = 485 nm).

The Saito group reported the synthesis of triphenylenes containing externally bridging S, Si and Sn heteroatoms (**111–113**; Scheme 9).[117] In each case the heteroatom was installed by initially lithiating acidic positions about the triphenylene scaffold with

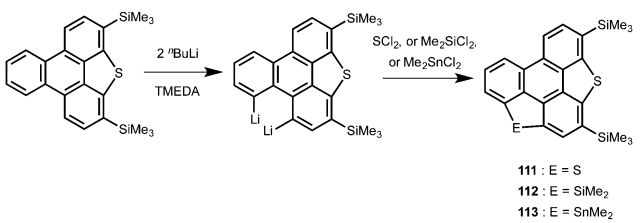

Scheme 9 Synthesis of heteroatom-bridged triphenylenes.

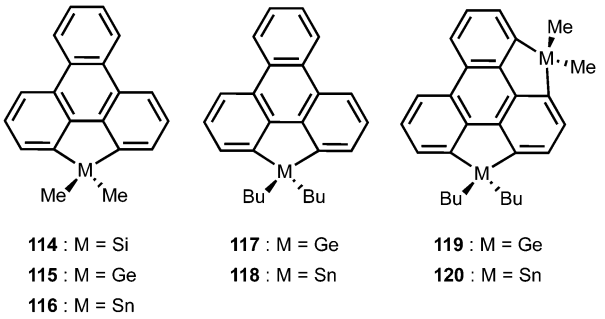

Fig. 9 Heterosummanenes reported by Saito and coworkers.

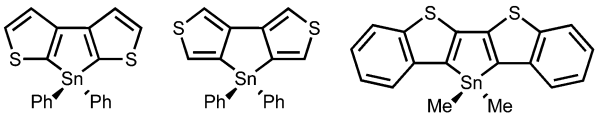

Fig. 10 Dithienostannole structural isomers (**121** and **122**) and the di(benzo[*b*]-thieno)stannole **123**.

an ^{n}BuLi/TMEDA (TMEDA = tetramethylethylenediamine) combination, followed by addition of the element dihalides SCl_2, Me_2SiCl_2 and Me_2SnCl_2. The Si and Sn analogues (**112** and **113**) have nearly identical absorbance spectra, and accordingly, computations indicate no orbital participation from the Si or Sn atoms to the HOMO and LUMO states. Building upon this work, Saito and coworkers reported the synthesis of a series of Group 14 element heterosumanenes in 2012 (Fig. 9).[118] Each fused polycycle exhibited strong UV light absorption from 250 to 290 nm, while the stannole derivatives (**116**, **118** and **120**) showed broad emission maxima at 370 nm, corresponding to violet-blue emission; the Si and Ge analogues also showed photoluminescence at 350 to 385 nm in solution.

The dithienostannole structural isomers (**121** and **122**; Fig. 10) were each synthesized in 2009 by Saito.[119] Each compound was characterized by X-ray crystallography however no further comparative study on their optoelectronic properties has been reported to date; Shimizu and coworkers also reported the dibenzothienostannole **123** in 2009.[120]

The Ohshita group has extensively explored bithiophenes as active components of conjugated materials, and in 2013 they prepared 1,1-diphenyl-3,6-bis(trimethylsilyl)dithienostannole (**124**) and di(benzo[*b*]-thieno)-1,1-diphenylstannole (**125**) (Fig. 11).[121] These fused heterocycles were synthesized from the reaction of the corresponding dilithiodithiophene and dilithiodibenzo[*b*]-thiophenes with Ph_2SnCl_2. Compound **125** displayed blue

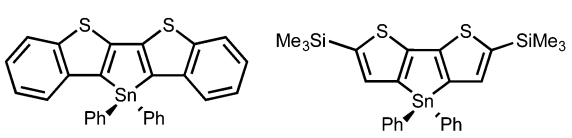

Fig. 11 Thiophene and benzothiophene-fused stannoles (**124** and **125**) prepared by Ohshita and coworkers.

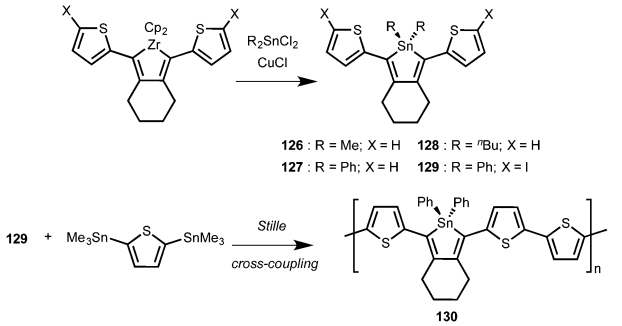

Scheme 10 Efficient synthesis of the polystannole **130** *via* Stille coupling.

photoluminescence when excited with 350 nm light in THF (λ_{em} = 410 nm) or when irradiated in crystalline form (λ_{em} = 422 nm); similar emission profiles were noted for **125**. Most interestingly, **125** exhibited crystallization-enhanced emission as a drastic increase in quantum yield was observed in the crystalline state (ϕ = 56%) relative to in THF solution (ϕ = 0.9%) or when **125** was deposited as an amorphous film (ϕ = 2.8%). This effect was not observed for **124** as the measured ϕ was comparable both in solution and in the crystalline state (29% in THF and 21% in the crystalline state). Analysis of the crystal structures of **124** and **125** gives some insight as to the source of the crystalline-induced emission in **125**. In compound **125** the only significant intermolecular interaction is π–π stacking between the phenyl groups, which was shown by computations to have a negligible contribution to emission. However **124** has notable π–π stacking interactions within 3.8 Å between the dithienostannole rings leading to some aggregation-caused quenching (ACQ).

In 2014, Staubitz and coworkers developed a selective Stille coupling procedure that enabled the preparation of the first high molecular weight polystannole.[122] The authors initially examined a series of thiophene-capped stannole model complexes (**126–128** in Scheme 10) and found that **127**, with Sn-phenyl linkages, was the most stable towards Stille coupling conditions. This led to the design of **129** as a possible monomer for polymerization *via* Stille coupling. Co-polymerization of **129** with bis(trimethylstannyl)thiophene yielded selective Stille coupling to form the air- and moisture-stable thiophene–stannole copolymer **130** as a dark purple solid in high molecular weight (M_w = 17.0 kDa) (Scheme 10). The UV-vis spectrum of **130** in chloroform showed a broad absorption peak at 536 nm, which was significantly red-shifted in comparison to the monomer **129** (λ_{max} = 441 nm). In addition the presence of stannole repeat units led to significant red-shifting of the absorption in relation to regioregular poly(3-hexylthiophene) (λ_{max} = 450 nm).[122] Spin-coated films of **130** displayed a further red-shift in $\lambda_{max.}$ to 585 nm due to enhanced thiophene–stannole ring co-planarity in the solid state. Luminescence measurements on **130** revealed extremely weak emission at 540 and 630 nm. The authors also estimated a band gap of 1.7 eV for **130** in the film state from the onset energy of light absorption, suggesting that these materials could be used in photovoltaic applications.

In a recent paper by the Jäkle group, the planar chiral dimethyl tin-bridged biferrocene (**131**; Fig. 12) was prepared,

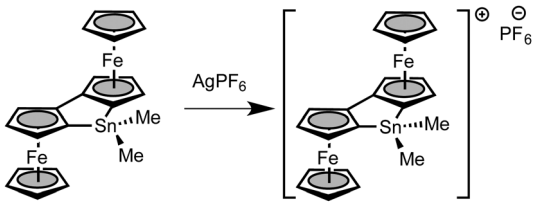

Fig. 12 Tin-bridged biferrocenes with their respective neutral and cationic forms.

and it was found that step-wise oxidation of the two Fe(II) centers to Fe(III) sites was possible.[123] Of note the mono-oxidized mixed valent Fe(II)/Fe(III) compound showed an intervalence charge transfer (IVCT) band in the near IR spectrum suggesting that electronic coupling between iron centers was occurring in solution. The authors mention a possible use of the oxidized analogues of **131** as redox-switchable chiral cations.

Lead

The incorporation of lead within possibly π-conjugated heterocycles is more challenging than the lighter analogues due to the increased lability of Pb–C bonds, leading to the common extrusion of lead metal from target cyclic species. Despite this inherent challenge, van Beelen and coworkers succeeded in isolating the air- and moisture-stable 1,1-dimethyl-2,3,4,5-tetraphenylplumbole (**134**) in 1978 from the reaction of dilithiotetraphenylbutadiene with Me_2PbBr_2 Scheme 11.[124] When this dilithiatedbutadiene was combined with $PbCl_2$, disproportionation occurred to yield a spiroplumbole (with Pb(IV) centers) and presumably lead metal. Soon after, the same group prepared a series of benzoplumboles and spiro-cycles (**133–152**; Scheme 11).[125,126]

The first crystallographic structure determinations of plumboles appeared in a 2010 study by Saito.[127] In this report, both the structures of hexaphenylplumbole $Ph_2PbC_4Ph_4$ (**137**) as well as

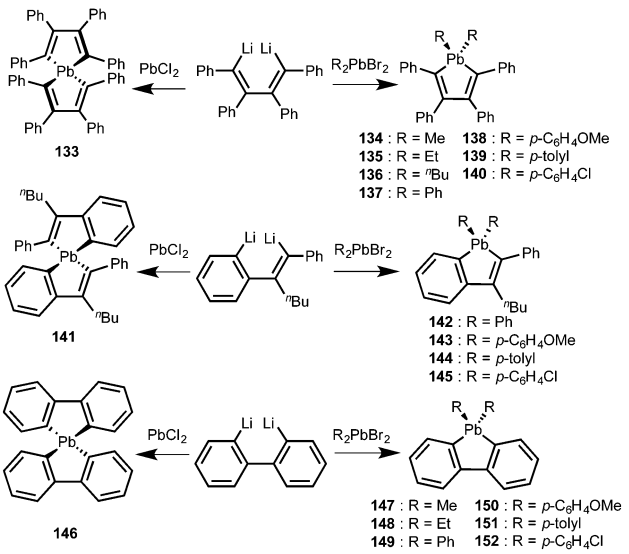

Scheme 11 Synthesis of arylated plumbole and spiroplumboles by van Beelen.

its spiro analogue $Pb(C_4Ph_4)_2$ (**133**) were determined; the general synthetic route used by the Saito group followed prior chemistry outlined by van Beelen *et al.* (Scheme 11).[124,125] As noted in other Group 14 metalloles, the absorption spectra for the hexaphenylplumbole (**137**) and the spiro-analogue (**133**) are similar to those reported the lighter $Ph_2EC_4Ph_4$ heterocycles (E = Si, Ge or Sn).[128] This observation has been linked to light absorption stemming from π–π* transitions that are localized primarily within the butadiene moieties. Interestingly each of the reported plumboles by Saito showed photoluminescence at room temperature with emission maxima (λ_{em}) at 394 nm (**137**) and 404 nm (**133**). These λ_{em} values are significantly blue-shifted from those noted in the lighter element congeners (Si, Ge and Sn) where λ_{em} values fall in the narrow range of 486–496 nm (in acetonitrile);[128] it is unclear at this stage why blue-shifted emission maxima occur within these plumboles.

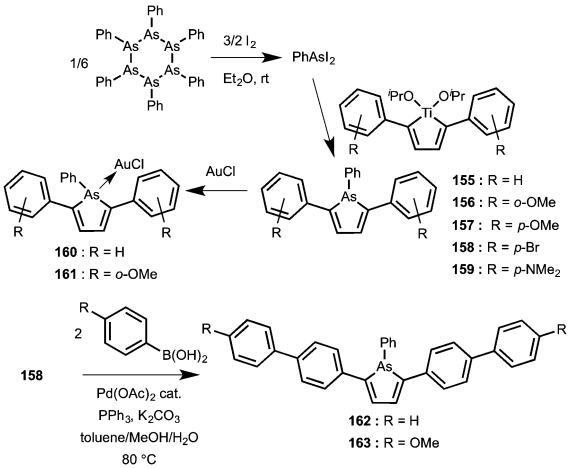

Scheme 13 Synthesis of 2,5-diarylarsoles *via* metallacycle transfer.

Group 15 heterocycles

The field of Group 15 element-containing π-conjugated materials is dominated by the lightest members of the series, nitrogen and phosphorus. The number of conjugated materials based upon the isolobal substitution of CH for N (*e.g.* benzene to pyridine) is vast and a discussion of the full impact of these important materials lies outside of the scope of this review. Briefly it is salient to cite some important review articles on phosphole and phosphabenzene chemistry,[129,130] including articles which describe the recent use of phosphole derivatives and their phosphine oxide analogues as light-emitting materials,[131] and as supports for metal-mediated catalysis.[132,133] As synthetic inorganic chemistry continues to grow as a field, new examples of heterocycles featuring arsenic, antimony and bismuth are surfacing in an increasingly frequent manner.[134]

Arsenic

Not surprisingly researchers have largely shied away from exploring the chemistry of this toxic element, however as will be seen, improvements in synthetic approaches have mitigated some of the pre-existing issues in this regard.

Braye *et al.* reported the synthesis of pentaphenylarsole $PhAsC_4Ph_4$ from the condensation reaction between 1,4-dilithioteraphenyl-1,3-butadiene and $PhAsCl_2$ in 1961.[135] The product was described as a yellow-green solid and fluorescent behavior was noted in this early report. Another efficient route to a prototypical arsenic-heterocycle (**154**) was reported by Fagan and Nugent in a landmark paper[136] (Scheme 12) wherein the readily accessible zirconacycle precursor $Cp_2ZrC_4Me_4$ (**153**) was

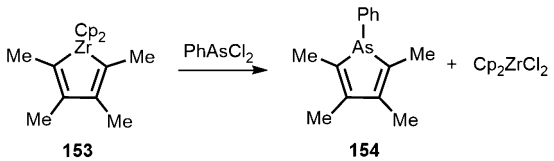

Scheme 12 Fagan and Nugent synthesis of an As-heterocycle *via* metallacycle transfer.

combined with $PhAsCl_2$ to instigate Zr/As atom exchange and form the air-stable arsole $PhAsC_4Me_4$ (**154**). Notably, this metallacycle transfer/atom exchange reaction can be extended to include most elements from the p-block.[136] While both of these methods provide formally 6π electron containing arsenic heterocycles in good yield, the use of volatile arsenic reagents is not ideal due to their known toxicity.

Recently the Naka group prepared a series of fluorescent 2,5-diarylarsoles from the reaction of *in situ* generated $PhAsI_2$ with titanacyclopentadienes (Scheme 13).[137] The authors highlight the importance of being able to conduct the synthesis without the use of volatile arsenic starting materials. Optical measurements revealed that the introduction of an arsenic atom in place of phosphorus did not significantly change the emission wavelength in chloroform solution; however a blue-shift of the emission in the solid state by about 20 nm (λ_{em} = 482 nm for **155**, 485 nm for **156**) in comparison to the known phosphole analogue (λ_{em} = 504 nm) was observed. Notably the arsenic-based heterocycles **155** and **156** are also more stable in the presence of oxygen in comparison to the corresponding phospholes. One possible explanation for this observation is the expected increase in s-character of the lone pair at As in relation to P, leading to an increased reluctance of arsenic to undergo oxidation. It was also found that **155** and **156** both form the stable 1 : 1 adducts with AuCl, **160** and **161**, respectively (Scheme 13). Upon binding gold, an increase of the overall quantum yield of the arsoles in chloroform solution was found (up to a value of 86% for **160**) as well as a 20–40 nm red-shift in emission in both solution and the solid state.

Following up on their previous work, Naka and coworkers reported the further functionalization of their arsenic-based metalloles *via* Pd-catalyzed Suzuki–Miyaura cross-coupling (Scheme 13) to yield the biphenyl-capped species **162** and **163**.[138] This reaction highlights a main advantage of these As-heterocycles as their lighter phosphole congeners tend to poison the catalytic activity of the Pd complexes required for cross-coupling. A bathochromic shift in both the absorbance and emission of the arsoles transpires when electron-donating

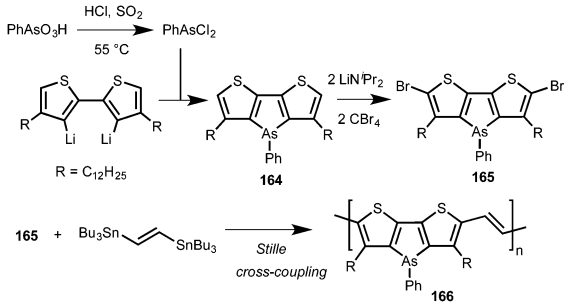

Scheme 14 Synthesis of the dithienoarsole polymer **166**.

groups are positioned on the thiophene rings (*e.g.* λ_{em} = 548 nm for **159** *vs.* 458 nm for the parent system **155**), as well as a corresponding increase in the energy of the HOMO (−4.67 eV for **159** *vs.* −5.59 eV for **155**). Interestingly, it was noticed that the emission colors of these arsenic heterocycles could be modified by mechanical stimuli such as grinding. A hypsochromic shift by about 10 nm was observed for compounds **155**, **156**, **157**, and **159** upon grinding, while this hypsochromic shift was more pronounced for **158** (*ca.* 50 nm).

A recent paper by Heeney *et al.* reported the synthesis of the first example of a dithienoarsole-containing polymer, **166.**[139] The synthesis was based on Stille cross-coupling polymerization as shown in Scheme 14. Using a different approach than Naka and coworkers, $PhAsCl_2$ was first generated *in situ* from phenylarsonic acid $PhAsO_3H_2$ and then reacted with a dodecyl-functionalized dilithiated bithiophene to form the required arsenic heterocycle **164**. Compound **164** was then brominated to give the air-stable monomer **165** (Scheme 14) which then was co-polymerized with *trans*-1,2-bis(tributylstannyl)ethene to yield **166** as a dark blue polymer. Calculations on a trimeric model of **166** indicate a highly planar backbone with very little twisting (less than 1°) between the dithienylarsole units and the adjacent olefinic spacers.

Antimony

In 2012, Ohshita *et al.* reported the synthesis and characterization of the first dithienylstiboles (Scheme 15).[140] Three variants were made (**167–169**) which demonstrated emission maxima ranging from 420 nm to 443 nm but with recorded quantum yields of only 1–2% in chloroform. The solid state emission spectrum for **169** afforded a notable red-shift in emission maxima by about 30 nm, suggesting that packing effects influenced the wavelength of emission. The stiboles were stable to ambient conditions, but decomposed upon continuous UV irradiation for one hour. In the case of **169** small amounts of naphthalene and bis(benzo[*b*]-thiophene) were detected after decomposition, suggesting that Sb–C bond scission was leading to loss of antimony metal upon irradiation. The authors also conducted DFT calculations to compare the HOMO and LUMO energies of dithienometalloles containing S, Sb, or Bi and found that the resulting computed energy levels remained largely invariant to the nature of the heteroatom present.

Bismuth

In 2006, Chujo and coworkers successfully prepared the polybismole **177**, the first well-defined polymer containing bismuth

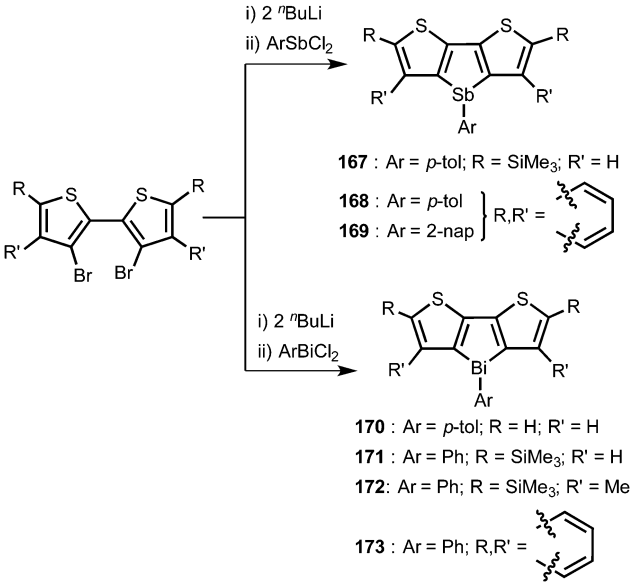

Scheme 15 Synthesis of dithienostiboles and dithienobismoles (**167–173**).

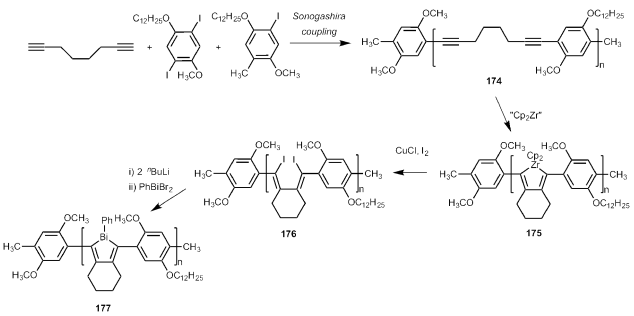

Scheme 16 Synthesis of the luminescent bismole-containing polymer **177**.

as an integral (main chain) component.[141,142] Incorporation of bismuth into a polymer was accomplished in the final step of a series of post-polymerization modification reactions outlined in Scheme 16. To begin, the polydiyne **174** was synthesized by Sonogashira coupling; the use of end-capping agents was used to control the resulting molecular weights and engender solubility for subsequent reaction chemistry. With the polydiyne **174** in hand, the authors conducted zirconium-mediated cyclization of the alkyne units to form the air- and moisture-sensitive polyzirconacycle **175**. This metallopolymer was treated with I_2 to extrude Cp_2ZrI_2 and yield a stable polydiiodobutadiene **176**, which was lithiated and subsequently reacted with $PhBiBr_2$ to form the target bismole–arene polymer **177**. Polymer **177** displayed photoluminescence with λ_{em} = 440 nm (λ_{ex} = 310 nm) in CH_2Cl_2 and a quantum efficiency approaching 13%. The authors did not comment on whether or not photoluminescence was possible for **177** in the solid state. The nature of the luminescence of **177** in CH_2Cl_2 remains to be confirmed as no lifetime measurements were taken, however the small Stokes shift noted suggests that the emission is fluorescence-based.

Following a pre-established synthetic route for yielding antimony-containing heterocycles, Ohshita and coworkers prepared a

series of dithienylbismoles **170–173** (Scheme 15).[143] The optical data for these fused heterocycles were similar to known silole analogues[47,144] with DFT studies revealing minimal participation from Bi to the HOMO states. Compounds **170–173** exhibited red photoluminescence in $CHCl_3$ with a sharp band at *ca.* 400 nm accompanied by a broad emission peak from 600–640 nm that was assigned to phosphorescence; in line with this postulate, the long wavelength emission was quenched in the presence of oxygen. In addition, self-quenching of phosphorescence (triplet–triplet annihilation) occurred in the solid state for the relatively planar bismoles **170** and **173**, while some phosphorescence was preserved in the $-SiMe_3$ capped heterocycles **171** and **172** (albeit with ϕ values below 0.2%). In the case of these silylated dithienobismoles, it is likely that close intermolecular contacts are suppressed by the presence of hindered $-SiMe_3$ groups, thus preventing complete triplet–triplet annihilation.

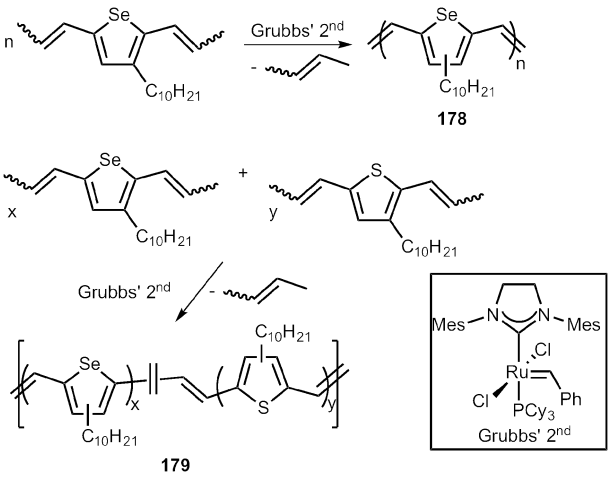

Scheme 17 Synthesis of **178** and **179** *via* ADMET polymerization.

Group 16 heterocycles

Selenium

In the domain of Se-containing π-conjugated materials, five-membered selenophenes have dominated the landscape. The seminal work by Bendikov has had a large effect on the overall experimental and theoretical understanding of selenophene polymers and oligomers, with their research laying the foundation for further explorations in this field.[145] Recently the Seferos group has published a review on the incorporation of selenophenes into electronic materials.[146] Herein we will describe developments of selenium-containing π-conjugated materials with optoelectronic applications that have emerged since Seferos' review.

Zhang and Qin synthesized two selenium-containing polymers with vinyl linkages, one containing only selenophene linkers (**178**) and one with randomly co-polymerized selenophene and thiophene functionalities (**179**).[147] They gained entry to these interesting materials by subjecting the reactive monomer, 3-decyl-2,5-dipropenylselenophene, to acyclic diene metathesis (ADMET) polymerization using Grubbs' 2nd generation catalyst in 1,3,5-trichlorobenzene at 90 °C. They also used dynamic vacuum to remove the 2-butene by-product as it formed, thus driving the reaction to completion (Scheme 17). Compound **178** was isolated in a 38% yield as a black solid, with an M_n of 14 300 g mol^{-1} and polydispersity index (PDI) of 1.8. The random co-polymer (**179**) was obtained by exposing a mixture of selenophene and thiophene monomers to similar ADMET conditions as used to prepare **178**. Co-polymer **179** displays red-shifted light absorption (λ_{max} = 597 nm) when compared to a related thiophene–vinylene (λ_{max} = 584 nm); as expected, **178** with entirely selenium-containing chalcogenophenes along the polymer backbone showed the most red-shifted absorption amongst the series with a λ_{max} of 617 nm. It would be of interest to see if such polymers could yield luminescence.

Al-Hashimi, Heeney and coworkers reported the Stille co-polymerization of 2,5-dibromo-3-dodecylselenophene with

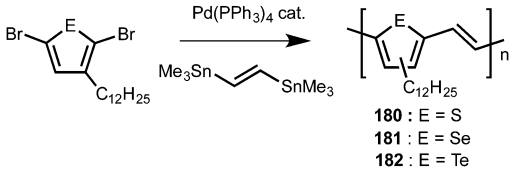

Scheme 18 Synthesis of polymers **180**, **181** and **182** *via* Stille coupling.

E-1,2-bis(tributylstannyl)ethylene to yield the vinylene–selenophene-containing co-polymer **181** (Scheme 18) in a 53% yield with an M_n of 12 000 g mol^{-1} (PDI = 2.0).[148] In line with prior studies in the field, progressive red-shifts in absorption were found when the heteroatom within the chalcogenophenes were changed from S to Se to Te with λ_{max} values of 572 to 613 to 653 nm, respectively for thin films of each vinylene-copolymer **180** to **182**. The charge carrier mobility of the selenophene analogue **181** was also investigated in conjunction with their use in TFTs. Polymer **181** was incorporated into three different device architectures, including bottom gate/top contact (BG/TC), bottom gate/bottom contact (BG/BC), and top gate/bottom contact (TG/BC) arrangements with field effect mobilities of 3.6×10^{-4}, 0.02 and 0.05 cm^2 V^{-1} s^{-1} respectively. The authors note that all polymers in this study (**180**, **181**, and **182**) were found to be p-type semiconductors and that the selenophene polymer consistently displayed the highest mobility across all devices.

Cheng and coworkers developed a series of tricyclic biselenophene based materials (Fig. 13).[149] These species consisted of dibrominated-biselenophene frameworks in combination with

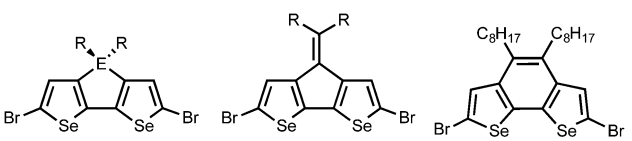

Fig. 13 Structure of the fused diselenoles **183–188**.

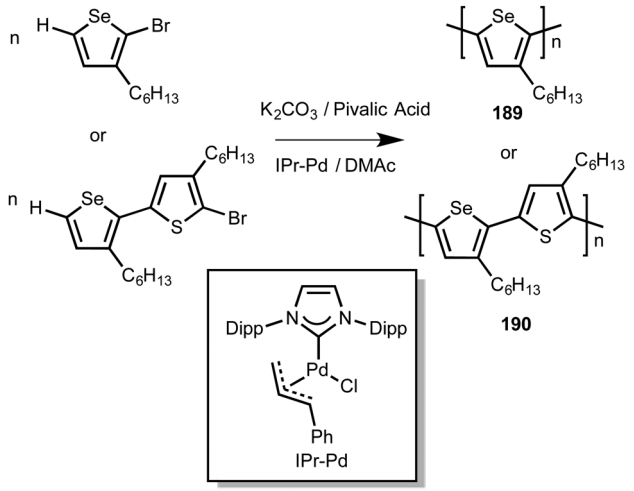

Scheme 19 Direct arylation polymerization yield **189** and **190**; Dipp = 2,6-$^{i}Pr_2C_6H_3$.

either sp^3-hybridized $-ER_2-$ linkages (E = Si or Ge; **183** and **184**), a three-coordinate octylamine bridge (**185**), or unsaturated exocyclic (**186** and **187**) and endocyclic (**188**) linkers. These compounds were all found to be photoluminescent, with the diselenogermole **184** showing the longest wavelength of blue light emission (476 nm), unfortunately no quantum yields were determined for compounds **183–188**. Due to the presence of polymerizable end-capping bromine substituents, these compounds represent promising building blocks for the fabrication of conjugated polymers. In this regard, Heeney and coworkers have incorporated diselenogermole donor-units into extended structures to yield polymers for BHJSC applications (*vide supra*).[93]

In 2015 Cheng *et al.* were able to form the regioregular selenophene-containing polymers **189** and **190** *via* palladium catalyzed direct-arylation polymerization (Scheme 19).[150] Polymer **189** could be prepared using either $Pd(OAc)_2$ or NHC–Pd catalysts (NHC = N-heterocyclic carbene) starting from 2-bromo-3-hexylselenophene as a monomer. Under the conditions employed, it was found that polymer precipitation occurred readily leading to incomplete monomer conversions and polymer M_n values consistently below 9000 g mol^{-1}. In an attempt to increase polymer solubility, the thiophene–selenophene copolymer **190** was prepared using related arylation polymerization (Scheme 19) and accordingly a higher molecular weight (M_n = 20 000 g mol^{-1}) was obtained due to decreased intermolecular interactions between the thiophene and selenophene repeat units. However incorporation of thiophene co-monomers in **190** led to a slight increase in optical band gap as reflected by UV-vis spectroscopy [λ_{max} (film) = 550 nm in **190** *vs.* 562 nm in **189**; similar trends were noted in solution].

The Haley group have recently prepared the indacenediselenophene **191** and the diindenoselenophene **192** (Fig. 14).[151] Compound **191** absorbs maximally at 577 nm, while the diindenoselenophene **192** displays vibronic features in the 350–500 nm region as well as another low energy absorption in the near IR at 675 nm. Both **191** and **192** are non-emissive as are related organic indenofluorenes.[152]

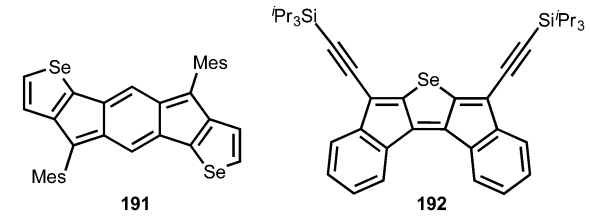

Fig. 14 Structures of **191** and **192**.

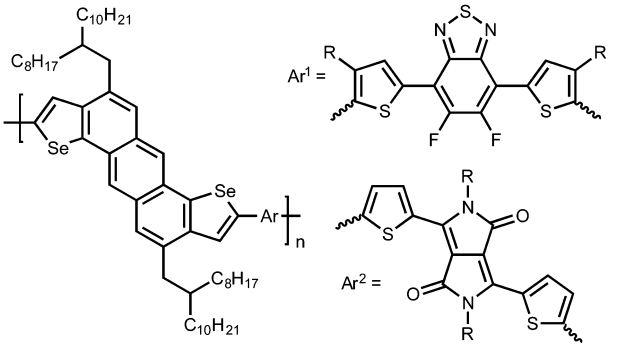

Fig. 15 The diselenoacene copolymers **193–196**.

A family of donor–acceptor copolymers (**193–196**) were prepared containing electron-rich fused anthradiselenophene units in combination with electron deficient repeat units (Ar^1 and Ar^2 in Fig. 15).[94] These polymers were prepared in 50–60% yield *via* Stille cross-coupling, and in line with a common practice in the field, long alkyl chains were placed about the periphery of these polymers to engender optimal solubility for film formation. These polymers were also incorporated into organic field effect transistors (OFETs) with a bottom gate/top contact arrangement with SiO_2 as the gate dielectric; each polymer was treated with $Cl_3Si–C_{18}H_{37}$ to form a self-assembled monolayer and then thermally annealed at 200 °C. Low mobilities were noted (up to 1.0 × 10^{-2} cm^2 V^{-1} s^{-1}), however excellent device on/off ratios approaching 10^8 (for **194**) were found. Polymers **193–196** were also incorporated BHJSCs yielding PCE values of up to 4.4% [with an ITO/PEDOT:PSS/polymer:$PC_{71}NM$/Ca/Al configuration].

Cabanetos, Blanchard and co-workers developed a selenophene (**197**) substituted at the 2- and 5-positions with an electron rich triphenylamine and an electron deficient dicyanovinyl group, respectively (Fig. 16).[153] As is expected for a push–pull π-system, strong visible light absorption was noted (ε = 36 800 M^{-1} cm^{-1}) with a λ_{max} in chloroform solution of 520 nm and a slightly red-shifted λ_{max} of 535 nm in the film state. A bulk heterojunction solar cell was fabricated containing **197** with a promising open circuit voltage (V_{OC}) of 0.95 V, however the low fill factor (FF) of 0.39 led to a modest overall PCE of 3.3%. The authors note that further device optimization of morphology, additives and interfaces is currently underway.

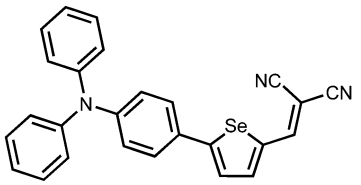

197

Fig. 16 The push–pull selenophene **197**.

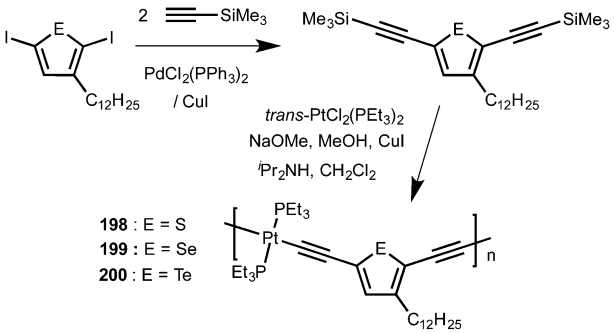

Scheme 20 Synthesis of polymers **198–200**.

The Seferos group was able to synthesize a series of platinum–bisacetylide chalcogenophene polymers (**198–200**).[154] The selenium-containing polymer (**199**, Scheme 20) was accomplished *via* the initial synthesis of the silyl-capped 2,5-bisalkyneselenophene followed by *in situ* deprotection–dehydrohalogenation polymerization with *trans*-$(Et_3P)_2PtCl_2$ to yield polymer **199** in a 47% yield with a M_n value of 30 900 g mol^{-1} (PDI = 2.08). This selenium-containing polymer **199** is also photoluminescent with blue-light emission centered at 452 nm and a measured quantum yield of 0.32%.

Seferos and co-workers have developed two co-polymer substructures (**201** and **202**) by coupling a bis(stannylated)-dithienogermole or a bis(stannylated)dithienosilole with dibromobenzoselenadiazole *via* Stille coupling (Scheme 21).[71] These polymers were obtained with molecular weights (M_n) as high as 33 000 g mol^{-1} and PDI values around 2.0. These benzoselenodiazole-*co*-polymers were then incorporated into BHJSCs with $PC_{71}BM$ as the acceptor material in the light harvesting/charge creation layer, with PCE values nearing 2.0% in unoptimized devices. The hole mobilities of **201** and **202** for undoped films were determined to be 1.53 × 10^{-4} and

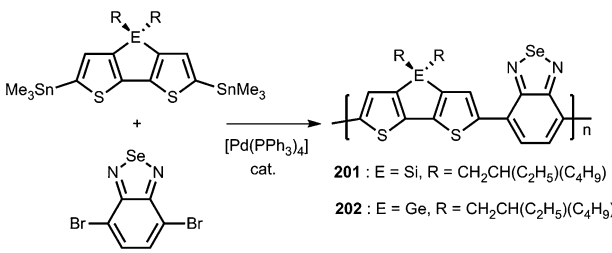

Scheme 21 Synthesis of the benzoselenodiazole co-polymers **201** and **202**.

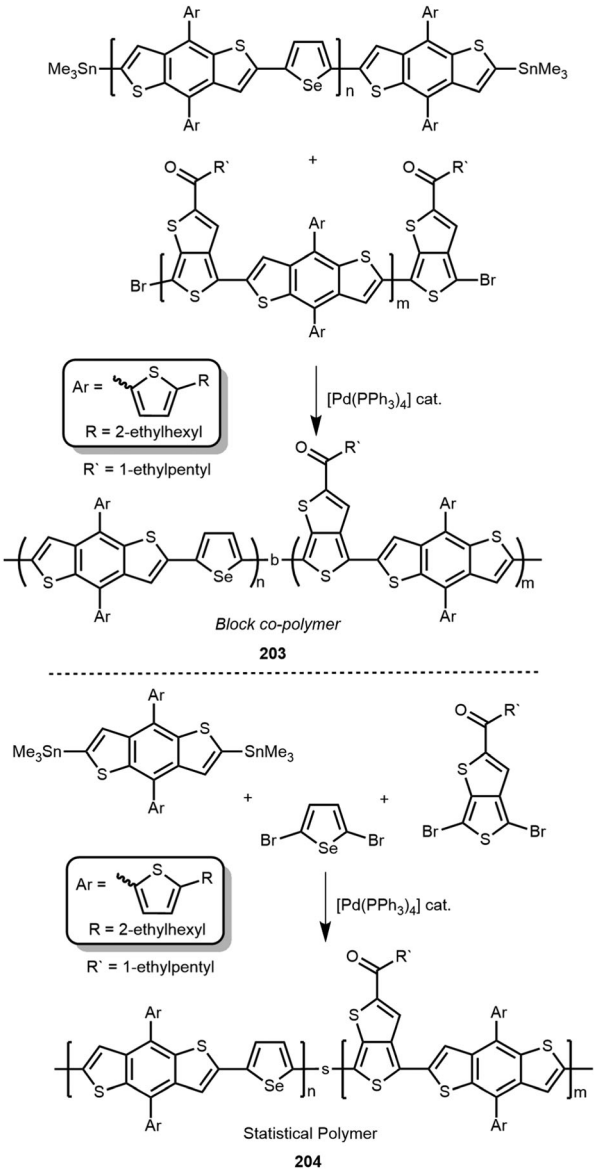

Scheme 22 Preparation of the selenophene-containing block co-polymer **203** and the statistical co-polymer **204**.

4.55 × 10^{-5} cm^2 V^{-1} s^{-1}, respectively. In related work, Seferos and coworkers prepared the selenophene-block copolymers **203** and **204** (Scheme 22); of note, polymer **203** was made by the direct polymer–polymer Stille coupling of pre-formed polyselenophene and polybenzobithiophene building blocks.[155] Meanwhile **204** was formed as a statistical mixture by combining three different monomers segments using Stille cross-coupling (Scheme 22). Polymer **203** was prepared with differing block ratios, however the overall molecular weights were around 20 000 g mol^{-1} and PDIs between 2.8–3.0; polymer **204** was prepared with a similar M_n of 19 200 g mol^{-1} and a corresponding PDI of 2.2. These polymers were both incorporated into an inverted bulk heterojunction solar cell with the ITO/ZnO/polymer:$PC_{71}BM$/MoO_3/Ag configuration; all polymers were blended in a 1 : 1.5 ratio with $PC_{71}BM$. For polymer **203**, the

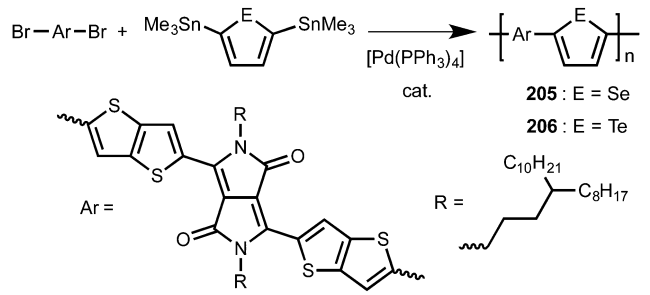

Scheme 23 Preparation of polymers **205** and **206**.

molecular weight/amount of co-polymer blocks used did not have a significant effect on solar cell outputs (PCE values approximately 5.8%). Also the overall PCE was not significantly higher in **203** in comparison to the random co-polymer **204** (PCE = 5.4%), yet having access block copolymer assemblies of controllable block ratios should give chemists an added tool in dialing-in optimal polymer–fullerene morphologies for BHJSCs.

Ashraf, Meager and coworkers have reported the use of 2,5-bis(trimethylstannyl)selenophene[156] to prepare polymer **205** bearing additional thieno[3,2-*b*]thiophene and diketopyrrolopyrrole subunits (Scheme 23).[157] Polymer **205** was obtained in a 65% yield with a high M_n value of 95 000 g mol^{-1} (PDI = 2.5); **205** also displayed efficient absorption in the near IR region with λ_{max} = 832 nm in the solid state. Polymer **205** was incorporated into a top gate/bottom contact (TG/BC) OFET yielding an impressive mobility of 1.6 cm^2 V^{-1} s^{-1}, a threshold voltage of −13 V and an on/off ratio of *ca.* 10^3. In addition, **205** was used to fabricate both conventional and inverted BHJSCs, with the best configuration being an inverted ITO/ZnO/polymer : $PC_{71}BM$; 1 : 2 ratio/MoO_3/Ag with an open circuit voltage of 0.56 V, a very high short circuit current (J_{SC}) of 21.5 mA cm^{-2}, a fill factor of 0.63, and an overall power conversion efficiency of 7.6%. Notably, the related tellurophene analogue **206** was also prepared with a slightly red-shifted λ_{max} (866 nm in solution and film) with a lower threshold voltage in TFTs of −8 V noted.[157]

Patra and coworkers recently developed an intriguing room temperature metal-free Br_2 catalyzed polymerization of selenophenes with a PEDOS-type structure (Scheme 24).[158] When R = H (**207**) the resulting insoluble black-colored polymer exhibited high levels of conductivity (2–4 S cm^{-1}), suggesting *in situ* doping of the resulting materials by bromine. Placement of dodecyl groups on the selenophene ring structure yielded a blue soluble polymer upon exposure to Br_2 (**208**) with a number average molecular weight (M_n) of *ca.* 5 × 10^3 g mol^{-1}.

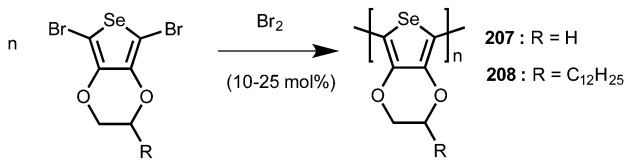

Scheme 24 Metal-free synthesis of polyselenophenes **207** and **208**.

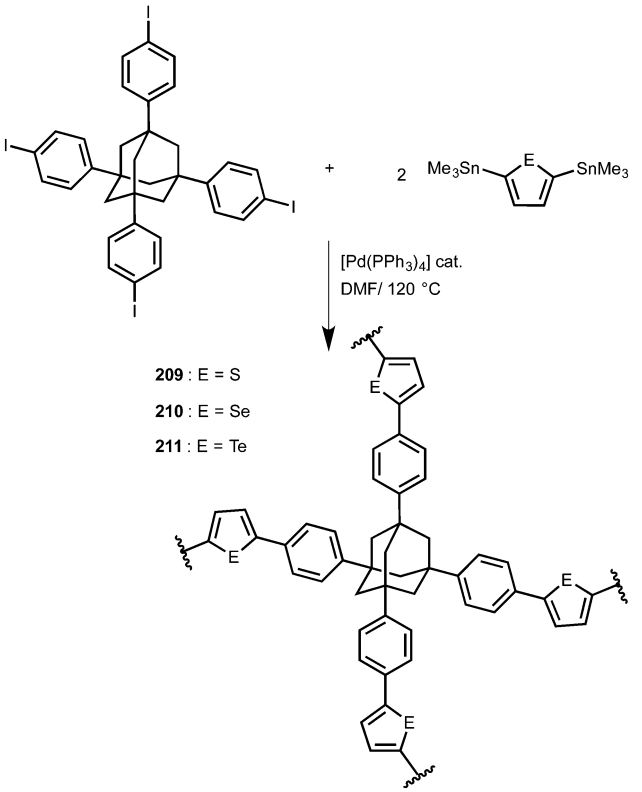

Scheme 25 Chalcogenophene framework materials prepared by the Seferos group.

In 2015, the Seferos group reported the preparation of a three-dimensional selenophene-containing organic framework (**210**) along with its corresponding thiophene (**209**) and tellurophene (**211**) analogues (Scheme 25).[159] The pore size in the selenophene organic framework **210** was estimated by modelling and BET (Brunauer–Emmett–Teller) measurements to be 42 Å and the surface area was found to be 478.8 m^2 g^{-1}, making this framework potentially useful as a mesoporous material. Both the thiophene (**209**) and selenophene (**210**) frameworks exhibited weak photoluminescence at λ_{max} = 542 nm and λ_{max} = 456 nm respectively, while the tellurium analogue is non-emissive (as is commonly encountered for such species). As expected, the UV-vis spectrum of the selenophene-containing organic framework **210** is red-shifted (350 nm) compared to the thiophene analogue (**209**; λ_{max} = 346 nm), while concurrently blue-shifted with respect to the Te analogue (**211**; λ_{max} = 366 nm), consistent with the calculated HOMO–LUMO gap for model compounds.

Tellurium

The synthesis of tetraphenyltellurophene TeC_4Ph_4 in 1961 by Braye *et al.* was the first example of a fully characterized substituted tellurophene complex.[135] Progress in the domain of tellurophene synthesis and reactivity has been summarized in various review articles,[160–162] and there have been reviews covering the incorporation of tellurophenes into polymeric structures.[163,164] More recently the Seferos group has published

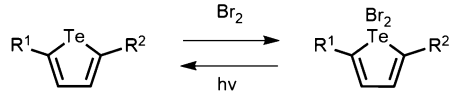

212 : $R^1 = R^2 = C_6H_5$ **221** : $R^1 = R^2 = C_6H_5$
213 : $R^1 = R^2 = C_6F_5$ **222** : $R^1 = R^2 = C_6F_5$
214 : $R^1 = R^2 = p\text{-}F_3C\text{-}C_6H_4$ **223** : $R^1 = R^2 = p\text{-}F_3C\text{-}C_6H_4$
215 : $R^1 = R^2 = p\text{-}O_2N\text{-}C_6H_4$ **224** : $R^1 = R^2 = p\text{-}O_2N\text{-}C_6H_4$
216 : $R^1 = R^2 = p\text{-}NC\text{-}C_6H_4$ **225** : $R^1 = R^2 = p\text{-}NC\text{-}C_6H_4$
217 : $R^1 = R^2 = p\text{-}t\text{Bu}\text{-}C_6H_4$ **226** : $R^1 = R^2 = p\text{-}t\text{Bu}\text{-}C_6H_4$
218 : $R^1 = R^2 = p\text{-}t\text{BuO}\text{-}C_6H_4$ **227** : $R^1 = R^2 = p\text{-}t\text{BuO}\text{-}C_6H_4$
219 : $R^1 = R^2 = p\text{-}Et_2N\text{-}C_6H_4$ **228** : $R^1 = R^2 = p\text{-}Et_2N\text{-}C_6H_4$
220 : $R^1 = p\text{-}O_2N\text{-}C_6H_4$, $R^2 = p\text{-}Bu_2N\text{-}C_6H_4$ **229** : $R^1 = p\text{-}O_2N\text{-}C_6H_4$, $R^2 = p\text{-}Bu_2N\text{-}C_6H_4$

Scheme 26 Reversible bromination of 2,5-diaryltellurophenes.

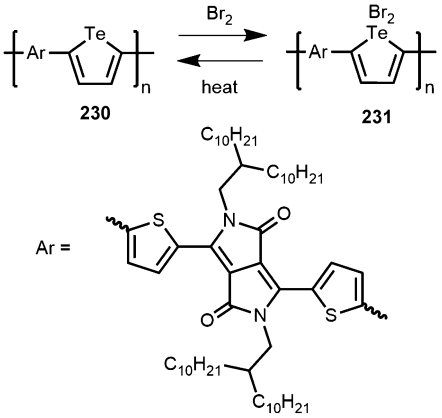

Scheme 27 Bromination of the polytellurophene **230**.

a comprehensive review on polytellurophenes for high performance applications,[165] while Rivard also described the use of tellurophenes as light-emitting materials in a separate review article.[166] As a result, we will review tellurium-containing π-conjugated materials with optoelectronic applications that have emerged since these most recent reviews were published.

Building upon their initial work containing dibromo- and dichloro-adducts of tellurophenes,[167] the Seferos group reported the photoreductive elimination of bromine, chlorine and quite impressively, fluorine, from 2,5-diphenyldihalotellurophenes.[168] They were able to demonstrate that the photoreductive elimination of bromine occurred rapidly with a 16.9% quantum efficiency when utilizing 2,3-dimethyl-1,3-butadiene (DMBD) as a halogen trap; such a process is key to the exploration of alternative methods of storing solar energy within chemical bonds (in this case a storage cycle based on hydrogen halides, HX).[169] Notably, the formal loss of F_2 from difluorotellurophenes is the only example of photoreductive elimination of fluorine from an inorganic compound (quantum yields up to 2.3%). The groups of Seferos and Scaiano combined efforts to explore the reactivity of the substituted 2,5-diaryltellurophenes **212–220** (Scheme 26) in detail.[170] These diaryltellurophenes contained a wide range of electron-donating and accepting units, with some aryl-tellurophene linkages prepared *via* an *ipso*-arylative cross coupling initially employed by Grubbs and coworkers to prepare polytellurophenes.[171,172] Compounds (**212–220**) were found to undergo oxidative addition of Br_2 to yield the dibromotellurophenes **221–229**. Each of these Te(IV) species underwent reversible photodebromination, with the most efficient loss of Br_2 occurring when electron-deficient $-C_6F_5$ groups were positioned onto a tellurophene. It was also noted that significant quenching of excited triplet states by oxygen competed with Br_2 loss, as determined by monitoring luminescence in the IR region from the singlet oxygen ($^1O_2$) generated after triplet quenching.[37]

Choi and coworkers[173] demonstrated that their previously synthesized polymer **230**[174] was able to undergo a similar reversible uptake of Br_2 (Scheme 27) as demonstrated previously by the Seferos group.[163] The color change in the polytellurophene produced upon bromination was used to develop a solid state optical sensor for elemental bromine. The Seferos group also noted reversible Br_2 uptake in the tellurophene-containing organic framework discussed previously in this review (**211**; Scheme 25), with a color change from green-brown to orange-red as $-TeBr_2-$ environments were formed; the release of bromine *via* photoreductive elimination studies on these 3D frameworks were not undertaken.

As mentioned in our section on selenium-containing π-systems, the Seferos group was able to synthesize a series of platinum–bisacetylide chalcogenophene polymers.[154] The tellurium-containing polymer (**200**, Scheme 20) was obtained in a 47% yield with an M_n value of 13 900 g mol^{-1} (PDI = 3.69). As expected for heavy atom substitution in conjugated materials, the absorption maximum (λ_{max}) for the tellurophene-containing polymer is significantly red-shifted (448 nm) compared to the Se (431 nm) and S (418 nm) analogues. This tellurium-containing polymer (**200**) shows weak fluorescence in the presence of air (λ_{max} = 460 nm; quantum yield = 0.06%), however upon degassing these chloroform solutions to remove dissolved oxygen, quenching of triplet emission was suppressed and a new phosphorescence emission peak at 671 nm emerged; this is a rare example of room temperature phosphorescence featuring a tellurophene.[175,176] In very interesting recent work, the Bonifazi laboratory have also noted phosphorescence in a series of benzo-1,3-chalcogenazoles, with one case of phosphorescence noted in the solid state.[177]

Earlier this year Seferos and coworkers[178] reported their findings related to the controlled synthesis of well defined, high molecular weight poly-3-alkyltellurophenes (**232–235**) utilizing catalyst transfer polycondensation methodology (Fig. 17). Specifically the role of side group branching was examined where it was found that the widely used 2-ethylhexyl groups had detrimental

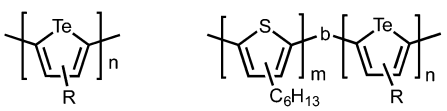

232 : R = 2-ethylhexyl **235** : R = 3-ethylheptyl
233 : R = 3-ethylheptyl
234 : R = 4-ethyloctyl

Fig. 17 Structures of the polytellurophenes **232–235**.

effects on the polymerization rate and the polymer quality, while placing ethyl branches at more remote 3- and 4-positions along the alkylchain led to improved molecular weight control and a red-shift in absorption. The authors attribute this to the decreased degree of twisting as the ethyl branch is moved further away from the heterocycle, resulting in increased effective conjugation between the tellurophene backbone units. The reported living polymerization of tellurophene also enabled the synthesis of the block copolymer, poly-3-hexylthiophene-*b*-poly-3-ethylheptyltellurophene (**235**).

Al-Hashimi, Heeney and coworkers reported a new synthesis of 2,5-dibromo-3-dodecyltellurophene and conducted a co-polymerization with *E*-1,2-bis(tributylstannyl)ethylene *via* Stille coupling to the poly-tellurophene–vinylene **182** (Scheme 18).[148] Polymer **182** was isolated in a 57% yield with an approximate M_n of 10 000 g mol^{-1} (PDI = 2.4). The charge carrier mobility of this polymer was also investigated for use in field effect transistors, however the production of high quality films was problematic due to its low solubility. Nonetheless, TFTs with two different device architectures, bottom gate/top contact, and top gate/bottom contact were prepared with field effect mobilities of 0.001 and 1.0 $\times$ 10^{-4} cm^2 V^{-1} s^{-1}, respectively. The authors note that the incorporating of tellurium does not exhibit an increase in mobility relative to its lighter element congeners, despite the possibility of close Te$\cdots$Te interactions. This is likely due to the poor film formation ability of this polymer and future work will focus on the side group modification to enhance TFT performance.

Conclusions

It was the intention of this review article to showcase the exciting chemical reactivity and promising optoelectronic properties one can attain when π-conjugated materials are designed with heavy main group elements as key components. Given the large number of very recent articles in this field, clearly there is a ''rising tide'' of collective research transpiring. Perhaps it is fitting to issue some parting challenges/goals to those exploring such inorganic–organic hybrid materials in the future.

By taking advantage of effective mixing between singlet and triplet excited states when heavy inorganic elements are present in π-conjugated materials, one could take advantage of long-lived exciton formation (up to the millisecond regime). This would lead to very long exciton diffusion lengths within photovoltaically active materials. Such species would be of great value to solar cell development[179] where pre-mature recombination of electron-holes (excitons) leading to energy loss is a major challenge, requiring intimate interfacial mixing of donor and acceptor materials at the nanoscale.

From the recent discovery of solid-state phosphorescence in heavy main group element-containing molecules, one could use this property to construct ''host-free'' LEDs if the existing challenge of enhancing charge migration through these next generation phosphors can be solved.[166] Furthermore due to large Stoke shift values inherent to phosphorescent materials, one could use emitting heavy element π-systems to eventually achieve stable near IR emission for bioimaging applications.[109]

Acknowledgements

The authors would like to thank NSERC of Canada for their on-going support (CREATE and Discovery Grants to E. R., Postgraduate Scholarships to S. M. P.). In addition the Killam Trust is acknowledged for funding a Postdoctoral Fellowship (M. P. B.). E. R. is grateful to Nagoya University and his host Prof. Shigehiro Yamaguchi for support in terms of a recent RCMS Visiting Professorship.

Notes and references

1 A. C. Grimsdale, K. Leok Chan, R. E. Martin, P. G. Jokisz and A. B. Holmes, *Chem. Rev.*, 2009, **109**, 897–1091.
2 J. W. Y. Lam and B. Z. Tang, *Acc. Chem. Res.*, 2005, **38**, 745–754.
3 N. C. Greenham, S. C. Moratti, D. D. C. Bradley, R. H. Friend and A. B. Holmes, *Nature*, 1993, **365**, 628–630.
4 G. Yu, J. Gao, J. C. Hummelen, F. Wudl and A. J. Heeger, *Science*, 1995, **270**, 1789–1791.
5 H. Shirakawa, E. J. Louis, A. G. MacDiarmid, C. K. Chiang and A. J. Heeger, *J. Chem. Soc., Chem. Commun.*, 1977, 578–580.
6 S. C. Rasmussen, S. J. Evenson and C. B. McCausland, *Chem. Commun.*, 2015, **51**, 4528–4543.
7 I. F. Perepichka, D. F. Perepichka, H. Meng and F. Wudl, *Adv. Mater.*, 2005, **17**, 2281–2305.
8 K. A. Mazzio and C. K. Luscombe, *Chem. Soc. Rev.*, 2015, **44**, 78–90.
9 Y. Liang and L. Yu, *Acc. Chem. Res.*, 2010, **43**, 1227–1236.
10 I. Osaka and R. D. McCullough, *Acc. Chem. Res.*, 2008, **41**, 1202–1214.
11 H. Sirringhaus, P. J. Brown, R. H. Friend, M. M. Nielsen, K. Bechgaard, B. M. W. Langeveld-Voss, A. J. H. Spiering, R. A. J. Janssen, E. W. Meijer, P. Herwig and D. M. de Leeuw, *Nature*, 1999, **401**, 685–688.
12 Y.-J. Cheng, S.-H. Yang and C.-S. Hsu, *Chem. Rev.*, 2009, **109**, 5868–5923.
13 J. Mei, N. L. C. Leung, R. T. K. Kwok, J. W. Y. Lam and B. Z. Tang, *Chem. Rev.*, 2015, **115**, 11718–11940.
14 A. M. Priegert, B. W. Rawe, S. C. Serin and D. P. Gates, *Chem. Soc. Rev.*, 2016, **45**, 922–953.
15 I. Manners, *Science*, 2001, **294**, 1664–1666.
16 X. Wang, G. Guerin, H. Wang, Y. Wang, I. Manners and M. A. Winnik, *Science*, 2007, **317**, 644–647.
17 X. Yan and C. Xi, *Acc. Chem. Res.*, 2015, **48**, 935–946.
18 K. K. Milnes, L. C. Pavelka and K. M. Baines, *Chem. Soc. Rev.*, 2016, **45**, 1019–1035.
19 E. Rivard, *Chem. Soc. Rev.*, 2016, **45**, 989–1003.
20 C. Präsang and D. Scheschkewitz, *Chem. Soc. Rev.*, 2016, **45**, 900–921.
21 E. Rivard and P. P. Power, *Inorg. Chem.*, 2007, **46**, 10047–10064.
22 R. C. Fischer and P. P. Power, *Chem. Rev.*, 2010, **110**, 3877–3923.
23 N. Tokitoh, *Acc. Chem. Res.*, 2004, **37**, 86–94.
24 A. J. Ashe III, *Acc. Chem. Res.*, 1978, **11**, 153–157.
25 C. Fan, W. E. Piers and M. Parvez, *Angew. Chem., Int. Ed.*, 2009, **48**, 2955–2958.
26 S. Yamaguchi, T. Shirasaka, S. Akiyama and K. Tamao, *J. Am. Chem. Soc.*, 2002, **124**, 8816–8817.
27 X. Yin, F. Guo, R. A. Lalancette and F. Jäkle, *Macromolecules*, 2016, **49**, 537–546.
28 F. Jäkle, *Chem. Rev.*, 2010, **110**, 3985–4022.
29 Z. M. Hudson and S. Wang, *Acc. Chem. Res.*, 2009, **42**, 1584–1596.
30 I. A. Adams and P. A. Rupar, *Macromol. Rapid Commun.*, 2015, **36**, 1336–1340.
31 C. R. Wade, A. E. J. Broomsgrove, S. Aldridge and F. P. Gabbaï, *Chem. Rev.*, 2010, **110**, 3958–3984.

32 A. Decken, F. P. Gabbaï and A. H. Cowley, *Inorg. Chem.*, 1995, **34**, 3853–3854.
33 A. Das, A. Hübner, M. Weber, M. Bolte, H.-W. Lerner and M. Wagner, *Chem. Commun.*, 2011, **47**, 11339–11341.
34 C. J. Berger, G. He, C. Merten, R. McDonald, M. J. Ferguson and E. Rivard, *Inorg. Chem.*, 2014, **53**, 1475–1486.
35 T. Matsumoto, K. Tanaka and Y. Chujo, *J. Am. Chem. Soc.*, 2013, **135**, 4211–4214.
36 For the use of the Maxm ligand to obtain Ga polymers, see: B. Bagh, J. B. Gilroy, A. Staubitz and J. Müller, *J. Am. Chem. Soc.*, 2010, **132**, 1794–1795.
37 D. F. Wilson, in *Oxygen Transport to Tissue XIV*, ed. W. Erdmann and D. F. Bruley, Springer US, Boston, MA, 1992, pp. 195–201.
38 T. Matsumoto, K. Tanaka and Y. Chujo, *Macromolecules*, 2015, **48**, 1343–1351.
39 W.-L. Yu, J. Pei, W. Huang, W.-L. Yu, J. Pei, Y. Cao and A. J. Heeger, *Chem. Commun.*, 1999, 1837–1838.
40 H. Yeo, K. Tanaka and Y. Chujo, *J. Polym. Sci., Part A: Polym. Chem.*, 2012, **50**, 4433–4442.
41 V. A. Kostyanovsky, D. K. Susarova, G. Adam, R. N. Lyubovskaya and P. A. Troshin, *Mendeleev Commun.*, 2013, **23**, 26–28.
42 M. Horie, L. A. Majewski, M. J. Fearn, C.-Y. Yu, Y. Luo, A. Song, B. R. Saunders and M. L. Turner, *J. Mater. Chem.*, 2010, **20**, 4347–4355.
43 C. Peppe and D. G. Tuck, *Polyhedron*, 1982, **1**, 549–552.
44 T. Matsumoto, K. Tanaka, K. Tanaka and Y. Chujo, *Dalton Trans.*, 2015, **44**, 8697–8707.
45 M. Montalti, A. Credi, L. Prodi and M. T. Gandolfi, *Handbook of Photochemistry*, 3rd edn, 2006, pp. 619–635.
46 S. Yamaguchi and K. Tamao, *Chem. Lett.*, 2005, **34**, 2–7.
47 J. Ohshita, *Macromol. Chem. Phys.*, 2009, **210**, 1360–1370.
48 W. W. H. Wong, J. F. Hooper and A. B. Holmes, *Aust. J. Chem.*, 2009, **62**, 393–401.
49 G. Lu, H. Usta, C. Risko, L. Wang, A. Facchetti, M. A. Ratner and T. J. Marks, *J. Am. Chem. Soc.*, 2008, **130**, 7670–7685.
50 Z. Zhao, B. He and B. Z. Tang, *Chem. Sci.*, 2015, **6**, 5347–5365.
51 M. Wang, X. Gu, G. Zhang, D. Zhang and D. Zhu, *Anal. Chem.*, 2009, **81**, 4444–4449.
52 M. Wang, D. Zhang, G. Zhang, Y. Tang, S. Wang and D. Zhu, *Anal. Chem.*, 2008, **80**, 6443–6448.
53 M. Wang, G. Zhang, D. Zhang, D. Zhu and B. Z. Tang, *J. Mater. Chem.*, 2010, **20**, 1858–1867.
54 J. J. McDowell, I. Schick, A. Price, D. Faulkner and G. Ozin, *Macromolecules*, 2013, **46**, 6794–6805.
55 T. L. Bandrowsky, J. B. Carroll and J. Braddock-Wilking, *Organometallics*, 2011, **30**, 3559–3569.
56 P. M. Beaujuge, C. M. Amb and J. R. Reynolds, *Acc. Chem. Res.*, 2010, **43**, 1396–1407.
57 C. M. Amb, S. Chen, K. R. Graham, J. Subbiah, C. E. Small, F. So and J. R. Reynolds, *J. Am. Chem. Soc.*, 2011, **133**, 10062–10065.
58 C. E. Small, S.-W. Tsang, S. Chen, S. Baek, C. M. Amb, J. Subbiah, J. R. Reynolds and F. So, *Adv. Energy Mater.*, 2013, **3**, 909–916.
59 C. E. Small, S. Chen, J. Subbiah, C. M. Amb, S.-W. Tsang, T.-H. Lai, J. R. Reynolds and F. So, *Nat. Photonics*, 2012, **6**, 115–120.
60 I. Constantinou, T.-H. Lai, D. Zhao, E. D. Klump, J. J. Deininger, C. K. Lo, J. R. Reynolds and F. So, *ACS Appl. Mater. Interfaces*, 2015, **7**, 4826–4832.
61 S. Chen, C. E. Small, C. M. Amb, J. Subbiah, T.-h. Lai, S.-W. Tsang, J. R. Manders, J. R. Reynolds and F. So, *Adv. Energy Mater.*, 2012, **2**, 1333–1337.
62 R. Casalini, S. W. Tsang, J. J. Deininger, F. A. Arroyave, J. R. Reynolds and F. So, *J. Phys. Chem. C*, 2013, **117**, 13798–13804.
63 J. Ohshita, M. Miyazaki, F.-B. Zhang, D. Tanaka and Y. Morihara, *Polym. J.*, 2013, **45**, 979–984.
64 J. Ohshita, M. Miyazaki, D. Tanaka, Y. Morihara, Y. Fujita and Y. Kunugi, *Polym. Chem.*, 2013, **4**, 3116–3122.
65 J. Ohshita, Y.-M. Hwang, T. Mizumo, H. Yoshida, Y. Ooyama, Y. Harima and Y. Kunugi, *Organometallics*, 2011, **30**, 3233–3236.
66 Y.-M. Hwang, J. Ohshita, Y. Harima, T. Mizumo, Y. Ooyama, Y. Morihara, T. Izawa, T. Sugioka and A. Fujita, *Polymer*, 2011, **52**, 3912–3916.
67 C. P. Yau, Z. Fei, R. S. Ashraf, M. Shahid, S. E. Watkins, P. Pattanasattayavong, T. D. Anthopoulos, V. G. Gregoriou, C. L. Chochos and M. Heeney, *Adv. Funct. Mater.*, 2014, **24**, 678–687.
68 J. S. Kim, Z. Fei, D. T. James, M. Heeney and J.-S. Kim, *J. Mater. Chem.*, 2012, **22**, 9975–9982.
69 Z. Fei, R. S. Ashraf, Z. Huang, J. Smith, R. J. Kline, P. D'Angelo, T. D. Anthopoulos, J. R. Durrant, I. McCulloch and M. Heeney, *Chem. Commun.*, 2012, **48**, 2955–2957.
70 X. Guo, N. Zhou, S. J. Lou, J. W. Hennek, R. Ponce Ortiz, M. R. Butler, P.-L. T. Boudreault, J. Strzalka, P.-O. Morin, M. Leclerc, J. T. López Navarrete, M. A. Ratner, L. X. Chen, R. P. H. Chang, A. Facchetti and T. J. Marks, *J. Am. Chem. Soc.*, 2012, **134**, 18427–18439.
71 G. L. Gibson, D. Gao, A. A. Jahnke, J. Sun, A. J. Tilley and D. S. Seferos, *J. Mater. Chem. A*, 2014, **2**, 14468–14480.
72 Q. Wang, S. Zhang, L. Ye, Y. Cui, H. Fan and J. Hou, *Macromolecules*, 2014, **47**, 5558–5565.
73 S. Yamaguchi, Y. Itami and K. Tamao, *Organometallics*, 1998, **17**, 4910–4916.
74 A. Karnezis, R. A. J. O'Hair and J. M. White, *Organometallics*, 2009, **28**, 4276–4282.
75 A. C. Spivey, C. J. G. Gripton and J. P. Hannah, *Curr. Org. Synth.*, 2004, **1**, 211–226.
76 A. C. Spivey, C.-C. Tseng, J. P. Hannah, C. J. G. Gripton, P. de Fraine, N. J. Parr and J. J. Scicinski, *Chem. Commun.*, 2007, 2926–2928.
77 A. C. Spivey, D. J. Turner, M. L. Turner and S. Yeates, *Synlett*, 2004, 111–115.
78 J. C. Bijleveld, V. S. Gevaerts, D. Di Nuzzo, M. Turbiez, S. G. J. Mathijssen, D. M. de Leeuw, M. M. Wienk and R. A. J. Janssen, *Adv. Mater.*, 2010, **22**, E242–E246.
79 H. Zhong, Z. Li, F. Deledalle, E. C. Fregoso, M. Shahid, Z. Fei, C. B. Nielsen, N. Yaacobi-Gross, S. Rossbauer, T. D. Anthopoulos, J. R. Durrant and M. Heeney, *J. Am. Chem. Soc.*, 2013, **135**, 2040–2043.
80 H. Zhong, Z. Li, E. Buchaca-Domingo, S. Rossbauer, S. E. Watkins, N. Stingelin, T. D. Anthopoulos and M. Heeney, *J. Mater. Chem. A*, 2013, **1**, 14973–14981.
81 Z. Fei, M. Shahid, N. Yaacobi-Gross, S. Rossbauer, H. Zhong, S. E. Watkins, T. D. Anthopoulos and M. Heeney, *Chem. Commun.*, 2012, **48**, 11130–11132.
82 R. S. Ashraf, B. C. Schroeder, H. A. Bronstein, Z. Huang, S. Thomas, R. J. Kline, C. J. Brabec, P. Rannou, T. D. Anthopoulos, J. R. Durrant and I. McCulloch, *Adv. Mater.*, 2013, **25**, 2029–2034.
83 L. Lu, T. Zheng, Q. Wu, A. M. Schneider, D. Zhao and L. Yu, *Chem. Rev.*, 2015, **115**, 12666–12731.
84 P.-C. Jwo, Y.-Y. Lai, C.-E. Tsai, Y.-Y. Lai, W.-W. Liang, C.-S. Hsu and Y.-J. Cheng, *Macromolecules*, 2014, **47**, 7386–7396.
85 J. Ohshita, M. Miyazaki, M. Nakashima, D. Tanaka, Y. Ooyama, T. Sasaki, Y. Kunugi and Y. Morihara, *RSC Adv.*, 2015, **5**, 12686–12691.
86 N. Allard, R. B. Aïch, D. Gendron, P.-L. T. Boudreault, C. Tessier, S. Alem, S.-C. Tse, Y. Tao and M. Leclerc, *Macromolecules*, 2010, **43**, 2328–2333.
87 Z. Fei, J. S. Kim, J. Smith, E. Buchaca-Domingo, T. D. Anthopoulos, N. Stingelin, S. E. Watkins, J.-S. Kim and M. Heeney, *J. Mater. Chem.*, 2011, **21**, 16257–16263.
88 U. Koldemir, S. R. Puniredd, M. Wagner, S. Tongay, T. D. McCarley, G. D. Kamenov, K. Müllen, W. Pisula and J. R. Reynolds, *Macromolecules*, 2015, **48**, 6369–6377.
89 A. Casey, Y. Han, Z. Fei, A. J. P. White, T. D. Anthopoulos and M. Heeney, *J. Mater. Chem. C*, 2015, **3**, 265–275.
90 J. Shaw, H. Zhong, C. P. Yau, A. Casey, E. Buchaca-Domingo, N. Stingelin, D. Sparrowe, W. Mitchell and M. Heeney, *Macromolecules*, 2014, **47**, 8602–8610.
91 Z. Fei, Y. Kim, J. Smith, E. Buchaca-Domingo, N. Stingelin, M. A. McLachlan, K. Song, T. D. Anthopoulos and M. Heeney, *Macromolecules*, 2012, **45**, 735–742.
92 D. Gendron, P.-O. Morin, P. Berrouard, N. Allard, B. R. Aïch, C. N. Garon, Y. Tao and M. Leclerc, *Macromolecules*, 2011, **44**, 7188–7193.
93 Z. Fei, R. S. Ashraf, Y. Han, S. Wang, C. P. Yau, P. S. Tuladhar, T. D. Anthopoulos, M. L. Chabinyc and M. Heeney, *J. Mater. Chem. A*, 2015, **3**, 1986–1994.
94 Y.-Y. Lai, H.-H. Chang, Y.-Y. Lai, W.-W. Liang, C.-E. Tsai and Y.-J. Cheng, *Macromolecules*, 2015, **48**, 6994–7006.

95 E.-i. Negishi, F. E. Cederbaum and T. Takahashi, *Tetrahedron Lett.*, 1986, **27**, 2829–2832.
96 B. L. Lucht, M. A. Buretea and T. D. Tilley, *Organometallics*, 2000, **19**, 3469–3475.
97 U. Rosenthal, A. Ohff, W. Baumann, A. Tillack, H. Görls, V. V. Burlakov and V. B. Shur, *Z. Anorg. Allg. Chem.*, 1995, **621**, 77–83.
98 H. J. Tracy, J. L. Mullin, W. T. Klooster, J. A. Martin, J. Haug, S. Wallace, I. Rudloe and K. Watts, *Inorg. Chem.*, 2005, **44**, 2003–2011.
99 J. Chen, H. Peng, C. C. W. Law, Y. Dong, J. W. Y. Lam, I. D. Williams and B. Z. Tang, *Macromolecules*, 2003, **36**, 4319–4327.
100 J. Chen, Z. Xie, J. W. Y. Lam, C. C. W. Law and B. Z. Tang, *Macromolecules*, 2003, **36**, 1108–1117.
101 Y. Yabusaki, N. Ohshima, H. Kondo, T. Kusamoto, Y. Yamanoi and H. Nishihara, *Chem. – Eur. J.*, 2010, **16**, 5581–5585.
102 J. Ohshita, K. Murakami, D. Tanaka, Y. Ooyama, T. Mizumo, N. Kobayashi, H. Higashimura, T. Nakanishi and Y. Hasegawa, *Organometallics*, 2014, **33**, 517–521.
103 T. P. I. Saragi, T. Spehr, A. Siebert, T. Fuhrmann-Lieker and J. Salbeck, *Chem. Rev.*, 2007, **107**, 1011–1065.
104 K.-H. Lee, J. Ohshita, D. Tanaka, Y. Tominaga and A. Kunai, *J. Organomet. Chem.*, 2012, **710**, 53–58.
105 R. Kondo, T. Yasuda, Y. S. Yang, J. Y. Kim and C. Adachi, *J. Mater. Chem.*, 2012, **22**, 16810–16816.
106 J. Ohshita, M. Nakamura and Y. Ooyama, *Organometallics*, 2015, **34**, 5609–5614.
107 O. Shynkaruk, G. He, R. McDonald, M. J. Ferguson and E. Rivard, *Chem. – Eur. J.*, 2016, **22**, 248–257.
108 G. L. Gibson, T. M. McCormick and D. S. Seferos, *J. Phys. Chem. C*, 2013, **117**, 16606–16615.
109 Y. You, *Curr. Opin. Chem. Biol.*, 2013, **17**, 699–707.
110 W. Uhl, S. Pelties, J. Tannert, B. J. Ravoo and E.-U. Würthwein, *Chem. – Eur. J.*, 2015, **21**, 2629–2637.
111 F. C. Leavitt, T. A. Manuel and F. Johnson, *J. Am. Chem. Soc.*, 1959, **81**, 3163–3164.
112 R. Gelius, *Chem. Ber.*, 1960, **93**, 1759–1768.
113 A. N. Chernega, A. J. Graham, M. L. H. Green, J. Haggitt, J. Lloyd, C. P. Mehnert, N. Metzler and J. Souter, *J. Chem. Soc., Dalton Trans.*, 1997, 2293–2304.
114 K. Geramita, J. McBee and T. D. Tilley, *J. Org. Chem.*, 2009, **74**, 820–829.
115 S. C. Cohen, D. E. Fenton, A. J. Tomlinson and A. G. Massey, *J. Organomet. Chem.*, 1966, **6**, 301–305.
116 S. C. Cohen and A. G. Massey, *J. Organomet. Chem.*, 1967, **10**, 471–481.
117 M. Saito, T. Tanikawa, T. Tajima, J. D. Guo and S. Nagase, *J. Organomet. Chem.*, 2010, **695**, 1035–1041.
118 T. Tanikawa, M. Saito, J. D. Guo, S. Nagase and M. Minoura, *Eur. J. Org. Chem.*, 2012, 7135–7142.
119 M. Saito, M. Shiratake, T. Tajima, J. D. Guo and S. Nagase, *J. Organomet. Chem.*, 2009, **694**, 4056–4061.
120 I. Nagao, M. Shimizu and T. Hiyama, *Angew. Chem., Int. Ed.*, 2009, **48**, 7573–7576.
121 D. Tanaka, J. Ohshita, Y. Ooyama, N. Kobayashi, H. Higashimura, T. Nakanishi and Y. Hasegawa, *Organometallics*, 2013, **32**, 4136–4141.
122 J. Linshoeft, E. J. Baum, A. Hussain, P. J. Gates, C. Näther and A. Staubitz, *Angew. Chem., Int. Ed.*, 2014, **53**, 12916–12920.
123 J. Chen, D. A. Murillo Parra, R. A. Lalancette and F. Jäkle, *Organometallics*, 2015, **34**, 4323–4330.
124 D. C. van Beelen, J. Wolters and A. van der Gen, *J. Organomet. Chem.*, 1978, **145**, 359–363.
125 D. C. van Beelen, J. Wolters and A. van der Gen, *Recl. Trav. Chim. Pays-Bas*, 1979, **98**, 437–440.
126 R. Gelius, *Angew. Chem.*, 1960, **72**, 322.
127 M. Saito, M. Sakaguchi, T. Tajima, K. Ishimura and S. Nagase, *Phosphorus, Sulfur Silicon Relat. Elem.*, 2010, **185**, 1068–1076.
128 J. Ferman, J. P. Kakareka, W. T. Klooster, J. L. Mullin, J. Quattrucci, J. S. Ricci, H. J. Tracy, W. J. Vining and S. Wallace, *Inorg. Chem.*, 1999, **38**, 2464–2472.
129 A. J. Ashe III, *Eur. J. Inorg. Chem.*, 2016, 572–574.
130 T. Baumgartner and R. Réau, *Chem. Rev.*, 2006, **106**, 4681–4727.
131 T. Baumgartner, *Acc. Chem. Res.*, 2014, **47**, 1613–1622.
132 Y. Matano and H. Imahori, *Acc. Chem. Res.*, 2009, **42**, 1193–1204.
133 K. Fourmy, D. H. Nguyen, O. Dechy-Cabaret and M. Gouygou, *Catal. Sci. Technol.*, 2015, **5**, 4289–4323.
134 G. He, O. Shynkaruk, M. W. Lui and E. Rivard, *Chem. Rev.*, 2014, **114**, 7815–7880.
135 E. H. Braye, W. Hübel and I. Caplier, *J. Am. Chem. Soc.*, 1961, **83**, 4406–4413.
136 P. J. Fagan and W. A. Nugent, *J. Am. Chem. Soc.*, 1988, **110**, 2310–2312.
137 M. Ishidoshiro, Y. Matsumura, H. Imoto, Y. Irie, T. Kato, S. Watase, K. Matsukawa, S. Inagi, I. Tomita and K. Naka, *Org. Lett.*, 2015, **17**, 4854–4857.
138 M. Ishidoshiro, H. Imoto, S. Tanaka and K. Naka, *Dalton Trans.*, 2016, 8717–8723.
139 J. P. Green, Y. Han, R. Kilmurray, M. A. McLachlan, T. D. Anthopoulos and M. Heeney, *Angew. Chem., Int. Ed.*, 2016, 7148–7151.
140 J. Ohshita, R. Fujita, D. Tanaka, Y. Ooyama, N. Kobayashi, H. Higashimura and Y. Yamamoto, *Chem. Lett.*, 2012, **41**, 1002–1003.
141 Y. Morisaki, K. Ohashi, H.-S. Na and Y. Chujo, *J. Polym. Sci., Part A: Polym. Chem.*, 2006, **44**, 4857–4863.
142 For a nice recent review on main group element-containing polymers, see: ref. 14.
143 J. Ohshita, S. Matsui, R. Yamamoto, T. Mizumo, Y. Ooyama, Y. Harima, T. Murafuji, K. Tao, Y. Kuramochi, T. Kaikoh and H. Higashimura, *Organometallics*, 2010, **29**, 3239–3241.
144 J. Chen and Y. Cao, *Macromol. Rapid Commun.*, 2007, **28**, 1714–1742.
145 A. Patra and M. Bendikov, *J. Mater. Chem.*, 2010, **20**, 422–433.
146 J. Hollinger, D. Gao and D. S. Seferos, *Isr. J. Chem.*, 2014, **54**, 440–453.
147 Z. Zhang and Y. Qin, *ACS Macro Lett.*, 2015, **4**, 679–683.
148 M. Al-Hashimi, Y. Han, J. Smith, H. S. Bazzi, S. Y. A. Alqaradawi, S. E. Watkins, T. D. Anthopoulos and M. Heeney, *Chem. Sci.*, 2016, **7**, 1093–1099.
149 Y.-C. Pao, Y.-L. Chen, Y.-T. Chen, S.-W. Cheng, Y.-Y. Lai, W.-C. Huang and Y.-J. Cheng, *Org. Lett.*, 2014, **16**, 5724–5727.
150 Y.-Y. Lai, T.-C. Tung, W.-W. Liang and Y.-J. Cheng, *Macromolecules*, 2015, **48**, 2978–2988.
151 J. L. Marshall, G. E. Rudebusch, C. L. Vonnegut, L. N. Zakharov and M. M. Haley, *Tetrahedron Lett.*, 2015, **56**, 3235–3239.
152 B. D. Rose, L. E. Shoer, M. R. Wasielewski and M. M. Haley, *Chem. Phys. Lett.*, 2014, **616–617**, 137–141.
153 A. Labrunie, Y. Jiang, F. Baert, A. Leliège, J. Roncali, C. Cabanetos and P. Blanchard, *RSC Adv.*, 2015, **5**, 102550.
154 A. K. Mahrok, E. I. Carrera, A. J. Tilley, S. Ye and D. S. Seferos, *Chem. Commun.*, 2015, **51**, 5475–5478.
155 D. Gao, G. L. Gibson, J. Hollinger, P. Li and D. S. Seferos, *Polym. Chem.*, 2015, **6**, 3353–3360.
156 S. Haid, A. Mishra, M. Weil, C. Uhrich, M. Pfeiffer and P. Bäuerle, *Adv. Funct. Mater.*, 2012, **22**, 4322–4333.
157 R. S. Ashraf, I. Meager, M. Nikolka, M. Kirkus, M. Planells, B. C. Schroeder, S. Holliday, M. Hurhangee, C. B. Nielsen, H. Sirringhaus and I. McCulloch, *J. Am. Chem. Soc.*, 2015, **137**, 1314–1321.
158 A. Patra, V. Agrawal, R. Bhargav, Shahjad, D. Bhardwaj, S. Chand, Y. Sheynin and M. Bendikov, *Macromolecules*, 2015, **48**, 8760–8764.
159 P.-F. Li, T. B. Schon and D. S. Seferos, *Angew. Chem., Int. Ed.*, 2015, **54**, 9361–9366.
160 C. R. B. Rhoden and G. Zeni, *Org. Biomol. Chem.*, 2011, **9**, 1301–1313.
161 I. D. Sadekov and V. I. Minkin, *Chem. Heterocycl. Compd.*, 2004, **40**, 834–853.
162 F. Fringuelli, G. Marino and A. Taticchi, in *Advances in Heterocyclic Chemistry*, ed. A. R. Katritzky and A. J. Boulton, Academic Press, 1977, vol. 21, pp. 119–173.
163 A. A. Jahnke and D. S. Seferos, *Macromol. Rapid Commun.*, 2011, **32**, 943–951.
164 M. Jeffries-El, B. M. Kobilka and B. J. Hale, *Macromolecules*, 2014, **47**, 7253–7271.
165 E. I. Carrera and D. S. Seferos, *Macromolecules*, 2015, **48**, 297–308.
166 E. Rivard, *Chem. Lett.*, 2015, **44**, 730–736.
167 E. I. Carrera, T. M. McCormick, M. J. Kapp, A. J. Lough and D. S. Seferos, *Inorg. Chem.*, 2013, **52**, 13779–13790.
168 E. I. Carrera and D. S. Seferos, *Dalton Trans.*, 2015, **44**, 2092–2096.
169 T. S. Teets and D. G. Nocera, *J. Am. Chem. Soc.*, 2009, **131**, 7411–7420.
170 E. I. Carrera, A. E. Lanterna, A. J. Lough, J. C. Scaiano and D. S. Seferos, *J. Am. Chem. Soc.*, 2016, **138**, 2678–2689.
171 Y. S. Park, T. S. Kale, C.-Y. Nam, D. Choi and R. B. Grubbs, *Chem. Commun.*, 2014, **50**, 7964–7967.

172 Y. S. Park, Q. Wu, C.-Y. Nam and R. B. Grubbs, *Angew. Chem., Int. Ed.*, 2014, **53**, 10691–10695.
173 M. Kaur, D. H. Lee, D. S. Yang, H. A. Um, M. J. Cho, J. S. Kang and D. H. Choi, *Dyes Pigm.*, 2015, **123**, 317–322.
174 M. Kaur, D. S. Yang, J. Shin, T. W. Lee, K. Choi, M. J. Cho and D. H. Choi, *Chem. Commun.*, 2013, **49**, 5495–5497.
175 G. He, W. Torres Delgado, D. J. Schatz, C. Merten, A. Mohammadpour, L. Mayr, M. J. Ferguson, R. McDonald, A. Brown, K. Shankar and E. Rivard, *Angew. Chem., Int. Ed.*, 2014, **53**, 4587–4591.
176 G. He, B. D. Wiltshire, P. Choi, A. Savin, S. Sun, A. Mohammadpour, M. J. Ferguson, R. McDonald, S. Farsinezhad, A. Brown, K. Shankar and E. Rivard, *Chem. Commun.*, 2015, **51**, 5444–5447.
177 A. Kremer, A. Fermi, N. Biot, J. Wouters and D. Bonifazi, *Chem. – Eur. J.*, 2016, **22**, 5665–5675.
178 S. Ye, M. Steube, E. I. Carrera and D. S. Seferos, *Macromolecules*, 2016, **49**, 1704–1711.
179 M. Tabachnyk, B. Ehrler, S. Gélinas, M. L. Böhm, B. J. Walker, K. P. Musselman, N. C. Greenham, R. H. Friend and A. Rao, *Nat. Mater.*, 2014, **13**, 1033–1038.